Pan-tropical prediction of forest structure from the largest trees

Jean-Francois Bastin, Ervan Rutishauser, James Kellner, Sassan Saatchi, Raphaël Pélissier, Bruno Hérault, Ferry Slik, Jan Bogaert, Charles de Canniere, Andrew M. Marshall, et al.

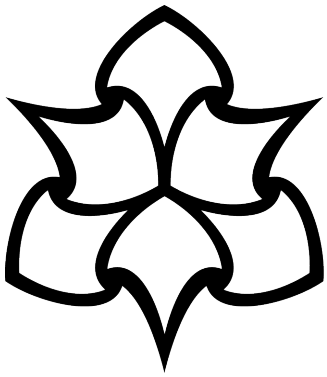

Title

Pan-tropical prediction of forest structure from the largest trees

Authors

Jean-François Bastin[1,2,3,4], Ervan Rutishauser[4,5],James R.Kellner[6,7], Sassan Saatchi[8], Raphael Pélissier[9], Bruno Hérault[10,11],Ferry Slik[12], Jan Bogaert[13], Charles De Cannière[2], Andrew R. Marshall[14,15,16], John Poulsen[17], Patricia Alvarez-Loyayza[18], Ana Andrade[19], Albert Angbonga-Basia[20], Alejandro Araujo-Murakami[21], Luzmila Arroyo[22], Narayanan Ayyappan[23,24], Celso Paulo de Azevedo[25], Olaf Banki[26], Nicolas Barbier[9], Jorcely G. Barroso[26], Hans Beeckman[27], Robert Bitariho[28], Pascal Boeckx[29], Katrin Boehning-Gaese[30,31], Hilandia Brandão[32], Francis Q.Brearley[33], Mireille Breuer Ndoundou Hockemba[34], Roel Brienen[35], Jose Luis C.Camargo[19], Sto[36], Benoit Cassart[37,38], Jérôme Chave[39], Robin Chazdon[40], Georges Chuyong[41], David B.Clark[42], Connie J.Clark[17], Richard Condit[43], Euridice N. Honorio Coronado[44], Priya Davidar[22],Thalès de Haulleville[13,27], Laurent Descroix[45],Jean-Louis Doucet[13],Aurelie Dourdain[46],Vincent Droissart[9],Thomas Duncan[47], Javier Silva Espejo[48], Santiago Espinosa[49],Nina Farwig[50],Adeline Fayolle[13], Ted R. Feldpausch[51], Antonio Ferraz[8], Christine Fletcher[36],Krisna Gajapersad[52], Jean-François Gillet[13], Iêda Leão do Amaral[32], Christelle Gonmadje[53], James Grogan[54], David Harris[55],Sebastian K.Herzog[56], Jürgen Homeier[57], Wannes Hubau[27], Stephen P. Hubbell[58,59], Koen Hufkens[29], Johanna Hurtado[60], Narcisse.G.Kamdem[61], Elizabeth Kearsley[62], David Kenfack[63], Michael Kessler[64], Nicolas Labrière[10,65], Yves Laumonier[10,66], Susan Laurance[67], William F.Laurance[68], Simon L. Lewis[35], Moses B. Libalah[61], Gauthier Ligot[13], Jon Lloyd[67,68], Thomas E. Lovejoy[69], Yadvinder Malhi[70], Beatriz S. Marimon[71], Ben Hur Marimon Junior[71], Emmanuel H.Martin[72], Paulus Matius[73], Victoria Meyer[8], Casimero Mendoza Bautista[74], Abel Monteagudo-Mendoza[75], Arafat Mtui[76], David Neill[77], Germaine Alexander Parada Gutierrez[78], Guido Pardo[79],Marc Parren[80], N. Parthasarathy[23],Oliver L. Phillips[35], Nigel C.A. Pitman[80], Pierre Ploton[9],Quentin Ponette[37], B.R.Ramesh[23], Jean-Claude Razafimahaimodison[81],Maxime Réjou-Méchain[9], Samir Gonçalves Rolim[82], Hugo Romero Saltos[83], Luiz Marcelo Brum Rossi[82], Wilson Roberto Spironello[32], Francesco Rovero[76],

Philippe Saner[84], Denise Sasaki[85], Mark Schulze[86], Marcos Silveira[87], James Singh[88], Plinio Sist[10,89], Bonaventure Sonke[61],J.Daniel Soto[90], Cintia Rodrigues de Souza[24], Juliana Stropp[91], Martin J.P. Sullivan[35], Ben Swanepoel[34], Hans ter Steege[25,92],John Terborgh[93,94],Nicolas Texier[95], T.Toma[96], Renato Valencia[97], Luis Valenzuela[75], Leandro Valle Ferreira[98], Fernando Cornejo Valverde[99], Tinde R Van Andel[25],Rodolfo Vasque[77], Hans Verbeeck[62],Pandi Vivek[22],Jason Vleminckx[100], Vincent A.Vos[79,101], Fabien H.Wagner[102], Warsudi[103],Verginia Wortel[104], Roderick J. Zagt[105],Donatien Zebaze[61]

1. Institute of Integrative Biology, Department of Environmental Systems Science, ETH Zürich, 8092 Zürich, Switzerland

2. Landscape Ecology and Plant Production System, Université libre de Bruxelles. CP264-2, B-1050 Bruxelles, Belgium

3. Affiliated during analysis and writing at NASA, Jet Propulsion Laboratory, California Institute of Technology, 4800 Oak Grove Drive, Pasadena, CA 91109, USA

4. Carboforexpert (carboforexpert.ch), 1248 Hermance, Switzerland

5. Smithsonian Tropical Research Institute, Box 0843-03092, Balboa, Ancon, Panama

6. Department of Ecology and Evolutionary Biology, Brown University, Providence, RI 02912, USA

7. Institute at Brown for Environment and Society, Brown University, Providence, RI 02912, USA

8. NASA, Jet Propulsion Laboratory, California Institute of Technology, 4800 Oak Grove Drive, Pasadena, CA 91109, USA

9. AMAP Lab, IRD, CIRAD, CNRS, INRA, Univ. Montpellier, Montpellier, France

10. Cirad, UR Forest & Societies, 34398 Montpellier Cedex 5, France

11. INPHB (Institut National Polytechnique Félix Houphouet Boigny), Yamoussoukro, Ivory Coast

12. Faculty of Science, Universiti Brunei Darusallam, Gadong, Brunei Darussalam

13. Gembloux Agro-Bio Tech, Université de Liège, B-5030 Gembloux, Belgium

14. CIRCLE, Environment Department, Wentworth Way, University of York, Heslington, York, YO10 5NG, UK

15. Tropical Forests and People Research Centre, University of the Sunshine Coast, QLD 4556, Australia

16. Flamingo Land Ltd., Kirby Misperton, YO17 6UX, UK

17. Nicholas School of the Environment, Duke University, PO Box 90328, Durham, NC 27708, USA

18. Field Museum of Natural History, Chicago, USA.

19. Biological Dynamics of Forest Fragment Project (BDFFP - INPA/STRI), Manaus - Amazonas, Brazil

20. Institut Facultaire des Sciences Agronomiques de Yangambi. DRC

21. Museo de Historia Natural Noel Kempff Mercado, Santa Cruz, Bolivia

22. Department of Ecology and Environmental Sciences, Pondicherry University, Kalapet, Pondicherry 605014, India

23. French Institute of Pondicherry (IFP), 11 Saint Louis Street, Pondicherry 605 001, India

24. Embrapa Amazônia Ocidental, Brazil

25. Naturalis Biodiversity Centre, PO Box 9517, 2300 RA Leiden, The Netherlands

26. Universidade Federal do Acre, Campus Floresta, Cruzeiro do Sul, Acre, Brazil

27. Service of Wood Biology, Royal Museum for Central Africa, Tervuren, Belgium

28. Institute of Tropical Forest Conservation, Mbarara University of Science and Technology, Uganda.

29. Isotope Bioscience Laboratory – ISOFYS, Ghent University, Belgium

30. Senckenberg Biodiversity and Climate Research Centre (BiK-F), Frankfurt am Main, Germany

31. Dept of Biological Sciences, Goethe Universität, Frankfurt am Main, Germany

32. National Institute for Amazonian Research (INPA), Manaus, Amazonas, Brazil

33. School of Science and the Environment, Manchester Metropolitan University, Chester Street, Manchester, M1 5GD, UK

34. Wildlife Conservation Society, New York, USA

35. School of Geography, University of Leeds, Leeds, UK

36. Malaysia Campus, Jalan Broga, Semenyih 43500, Selangor, Malaysia

37. UCL-ELI, Earth and Life Institute, Université catholique de Louvain, Louvain-la-Neuve BE-1348, Belgium

38. Ecole Régionale Post-universitaire d'Aménagement et de Gestion Intégrés des Forêts et Territoires Tropicaux, Kinshasa, DRC

39. Laboratoire Evolution et Diversité biologique, CNRS & Université Paul Sabatier, Toulouse 31062, France

40. Department of Ecology and Evolutionary Biology, University of Connecticut, Storrs, Connecticut 06268-3043, USA

41. Department of Botany and Plant Physiology, University of Buea, Cameroon

42. Department of Biology, University of Missouri-St Louis, Missouri, USA

43. Field Museum of Natural History and Morton Arboretum, Illinois, USA

44. Coronado, Inst. de Investigaciones de la Amazonia Peruana, Iquitos, Peru

45. ONF pôle R&D, Cayenne, France

46. Cirad, UMR EcoFoG (AgroParisTech, CNRS, Inra, Universite des Antilles, Universite de la Guyane), Kourou, French Guiana

47. Department of Botany and Plant Pathology, Oregon State University, Corvallis, OR 97331, USA

48. Departamento de Biología, Universidad de La Serena, Casilla 554 La Serena, Chile

49. Universidad Autónoma de San Luis Potosí, San Luis Potosí, México

50. Department of Conservation Ecology, Philipps-Universität Marburg, Karl-von-Frisch-Straße 8, 35032 Marburg, Germany

51. Geography, College of Life and Environmental Sciences, University of Exeter, Exeter, EX4 4RJ, UK

52. Conservation International Suriname, Paramaribo, Suriname

53. Department of Plant Biology, Faculty of science, University of Yaounde I, BP 812 Yaoundé, Cameroon

54. Mount Holyoke College Botanic Garden, South Hadley, MA 01075, USA

55. Royal Botanic Garden Edinburgh, Edinburgh EH3 5LR, UK

56. Museo de Historia Natural Alcide d'Orbigny, Cochabamba, Bolivia

57. Plant Ecology, University of Goettingen, Untere Karspuele 2, 37073 Goettingen, Germany

58. Department of Ecology and Evolutionary Biology, University of California, Los Angeles, California 90095, USA

59. Smithsonian Tropical Research Institute, Apartado 0843-03092, Balboa, Republic of Panama

60. Organization for Tropical Studies, Costa Rica

61. Plant Systematic and Ecology Laboratory, Higher Teacher's Training College, University of Yaoundé I, P.O. Box 047, Yaoundé, Cameroon.

62. CAVElab – Computational and Applied Vegetation Ecology, Ghent University, Belgium

63. CTFS-ForestGEO, Smithsonian Tropical Research Institute, MRC 166, NMNH, P.O. Box 37012, Washington, DC 20013-7012, USA

64. Department of Systematic and Evolutionary Botany, University of Zurich, Zollikerstrasse 107, Zurich 8008, Switzerland

65. AgroParisTech, Doctoral School ABIES, 19 Avenue du Maine, 75732 Paris Cedex 15, France

66. Center for International Forestry Research, Jl. CIFOR, Situ Gede, Bogor Barat 16115, Indonesia

67. Centre for Tropical Environmental and Sustainability Science, College of Science and Engineering, James Cook University, Cairns, Queensland 4870, Australia.

68. Department of Life Sciences, Imperial College London, SL5 7PY, Ascot, UK

69. Department of Environmental Science and Policy, George Mason University, Fairfax, VA, USA

70. Environmental Change Institute, School of Geography and the Environment, University of Oxford, Oxford, UK

71. Universidade do Estado de Mato Grosso, Campus de Nova Xavantina, Nova Xavantina, MT, Brazil

72. Udzungwa Ecological Monitoring Centre, Udzungwa Mountains National Park, Tanzania, Sokoine University of Agriculture, Morogoro, Tanzania

73. Escuela de Ciencias Forestales, Unidad Académica del Trópico, Universidad Mayor de San Simón, Sacta, Bolivia

74. Faculty of Forestry, Mulawarman University, Indonesia

75. Jardín Botánico de Missouri, Oxapampa, Pasco, Peru.

76. MUSE - Museo delle Scienze, Trento, Italy

77. Universidad Estatal Amazónica, Puyo, Pastaza, Ecuador

78. Museo de Historia Natural Noel Kempff Mercado, Santa Cruz, Bolivia

79. Universidad Autónoma del Beni, Riberalta, Bolivia

80. Science and Education, The Field Museum, 1400 South Lake Shore Drive, Chicago, Illinois 60605–2496, USA

81. Centre ValBio, Ranomafana, Madagascar

82. Embrapa Florestas, Colombo/PR, Brazil

83. Yachay Tech University, School of Biological Sciences and Engineering. Urcuquí, Ecuador

84. Department of Evolutionary Biology and Environmental Studies, University of Zurich, CH-8057 Zurich, Switzerland

85. Fundação Ecológica Cristalino Alta Floresta, Brazil

86. HJ Andrews Experimental Forest, PO Box 300, Blue River, OR 97413, USA

87. Museu Universitário, Universidade Federal do Acre, Rio Branco 69910-900, Brazil

88. Guyana Forestry Commission, Georgetown, Guiana

89. Forests and Societies, Univ. Montpellier, CIRAD, Montpellier, France

90. Museo de Historia Natural Noel Kempff Mercado, Santa Cruz, Bolivia

91. Institute of Biological and Health Sciences, Federal University of Alagoas, Maceió, Brazil

92. Systems Ecology, Free University, De Boelelaan 1087, Amsterdam, 1081 HV, Netherlands.

93. Florida Museum of Natural History and Department of Biology, University of Florida - Gainesville, Gainesville, FL 32611, USA

94. Department of Biology, James Cook University, Cairns, Australia

95. Laboratoire d'Evolution Biologique et Ecologie, Faculté des Sciences, Université libre de Bruxelles, CP160/12, 1050 Bruxelles, Belgium

96. Forestry and Forest Products Research Institute, Matsunosato 1, Tsukuba 305-8687, Japan

97. Escuela de Ciencias Biológicas, Pontificia Universidad Católica del Ecuador, Quito, Ecuador

98. Coordenação de Botânica, Museu Paraense Emilio Goeldi, Belém, Brazil

99. Andes to Amazon Biodiversity Program, Madre de Dios, Peru

100. Department of Integrative Biology, University of California, Berkeley, 1005 Valley Life Sciences Building 3140, Berkeley, CA 94720-3140, USA

101. Centro de Investigación y Promoción del Campesinado - Norte Amazónico, Riberalta, Bolivia

102. Remote Sensing Division, National Institute for Space Research - INPE, São José dos Campos 12227-010, SP, Brazil

103. The Center for Reforestation Studies in the Tropical Rain Forest (PUSREHUT), Mulawarman University, Jln. Kihajar Dewantara Kampus Gunung Kelua, Samarinda 75123, East Kalimantan, Indonesia

104. Center for Agricultural Research in Suriname (CELOS), Suriname

105. Tropenbos International, PO Box 232, Wageningen 6700 AE, The Netherlands

Abstract

Aim. Large tropical trees form the interface between ground and airborne observations, offering a unique opportunity to capture forest properties remotely. However, despite rapid development of metrics to characterize the forest canopy from remotely sensed data, a gap remains between aerial and field inventories. To close this gap, we propose a new pan-tropical model to predict plot-level forest structure properties and biomass from just the largest trees, as a proxy for the whole plot inventory.

Location. Pan-tropical

Method. Using a dataset of 867 plots distributed among 118 sites across the tropics, we tested the ability to predict quadratic mean diameter, basal area, Lorey's height and community wood density from the i^{th} largest trees, i.e. testing the cumulative information gathered from these i trees ranked by decreasing diameter. These tests served as a basis to select the optimal number of the largest trees and further predict plot-level biomass from a single model.

Result. Focusing on readily available information captured by airborne remote sensing, we show that measuring the largest trees in tropical forests enables unbiased predictions of plot and site-level forest structure. The 20 largest trees per hectare predicted quadratic mean diameter, basal area, Lorey's height and community wood density with 12%, 16%, 4% and 4% of relative error. Building on this result, we developed a new model to predict plot-level AGB from measurements of the 20 largest trees. This model allows an independent and unbiased prediction of biomass with 17.7% of error compared to ground estimates. Most of the remaining error is driven by differences in the proportion of total biomass held in medium size trees (50-70 cm), which shows some continental dependency with American tropical forests presenting the highest levels of total biomass share in these intermediate diameter classes.

Conclusion. Our approach provide new information on tropical forest structure and can be employed to generate accurately field estimates of tropical forest carbon stocks to support the calibration and validation of current and forthcoming space missions. It will reduce the cost of programs to monitor, report, and verify forest resources, and will contribute to scientific understanding of tropical forest ecosystems and response to climate change.

Introduction

The fundamental ecological function of large trees is well established for tropical forests. They offer shelter to a multiple organisms (Remm & Lõhmus, 2011; Lindenmayer *et al.*, 2012), regulate forest dynamics, regeneration (Harms *et al.*, 2000; Rutishauser *et al.*, 2010) and total biomass (Stegen *et al.*, 2011), and are important contributor to the global carbon cycle (Meakem *et al.*, 2017). Being major components of the canopy, the largest trees also suffer more than sub-canopy and understory trees from climate change, as they are directly exposed to variations in solar radiation, wind strength, temperature seasonality and relative air humidity (Laurance *et al.*, 2000; Nepstad *et al.*, 2007; Lindenmayer *et al.*, 2012; Thomas *et al.*, 2013; Bennett *et al.*, 2015; Meakem *et al.*, 2017). Because they are visible from the sky, large trees are ideal for monitoring forest responses to climate change via remote sensing (Bennett *et al.*, 2015; Asner *et al.*, 2017).

Large trees encompass a disproportionate fraction of total above-ground biomass (AGB) in tropical forests (Chave *et al.*, 2001), with some variations in their relative contribution to the total AGB among the tropical regions (Feldpausch *et al.*, 2012). In Central Africa, the largest 5% of trees, i.e. the 5% of trees with the largest diameter at 130 cm per area, store 50% of forest aboveground biomass on average (Bastin *et al.*, 2015). Consequently, the density of large trees largely explains variation in AGB at local (Clark & Clark, 1996), regional (Malhi *et al.*, 2006; Saatchi *et al.*, 2007), and continental scales (Stegen *et al.*, 2011; Slik *et al.*, 2013). Detailing the contribution of each single tree to the diameter structure, we showed previously that plot-level AGB can be predicted from a few large trees (Bastin *et al.*, 2015), with the measurement of the 20 largest trees per hectare being sufficient to estimate plot-level biomass with less than 15% errors in reference to ground estimates. These findings opened the possibility of measuring the largest trees to cost-effectively monitor forest biomass in Central Africa, rather than conducting full inventories of all size classes. Similarly, they suggested that remote sensing (RS) approaches should focus on the measurement of the largest trees, instead of properties of the entire forest.

Several efforts are underway to close the gap between remote sensing and field surveys (e.g. Jucker et al. 2016a, Coomes et al. 2017). However, field inventories still rely on exhaustive data collection, while remote sensing surveys provide a limited alternative for the following reasons. Existing RS approaches that provide predictions of biomass with less than 20% error for 1 ha plot size are either specific to the relationship between forest type and image/scene properties (Barbier *et al.*, 2011; Asner *et al.*, 2012; Barbier & Couteron, 2015), or require ground measurement of all trees above or equal to 10 cm of *D* for calibration (Asner *et al.*, 2012; Asner & Mascaro, 2014). Using mean canopy height extracted from active sensors (Mascaro *et al.*, 2011; Ho Tong Minh *et al.*, 2016), or canopy grain derived from optical images (Proisy *et al.*, 2007; Ploton *et al.*, 2012, 2017; Bastin *et al.*, 2014), the biomass is predicted from remote sensing with a typical error of only 10-20% compared to ground-based estimates, but is limited to the extent of the scene used. An interesting development to alleviate this spatial restriction lies in the 'universal approach', proposed by Asner et al. (2012) and further adapted in Asner and Mascaro (2014), in which plot-level biomass is predicted by a linear combination of ground-based and remotely-sensed metrics. The 'universal approach' relies upon canopy height metrics derived from radar or LiDAR (top of canopy height, TCH), and basal area (BA, i.e. the cross-sectional stem area) and community wood density (i.e. weighted by basal area, WD_{BA}) derived from full field inventories. AGB is then predicted as follows (Asner *et al.*, 2012):

$$AGB = aTCH^{b1}BA^{b2}WD_{BA}^{b3} \quad (1)$$

While generally performing better than approaches based solely on remote sensing of tree height (Coomes *et al.*, 2017), this model largely relies on exhaustive ground measurements (i.e. wood density and basal area of all trees above 10 cm of diameter at 130 cm, neither of which is measured using any existing remotely sensed data).

Recent advances in remote sensing allow the identification of single trees in the canopy (Ferraz *et al.*, 2016), estimation of adult mortality rates for canopy tree species (Kellner & Hubbell, 2017), description of the forest diameter structure (Stark *et al.*, 2015), depiction of crown and gap shapes (Coomes *et al.*, 2017), and even identification of some functional traits of canopy species (Asner *et al.*, 2017). Building upon this work, we test the capacity of metrics from the

largest trees that can be potentially derived using remote sensing to predict plot-level biomass (i.e. the summed AGB of all live trees D ≥10 cm in a plot). To this end, we tested the following model:

$$AGB = a(Dg_{LT\,i} H_{LT\,i} WD_{LT\,i})^{b1} \quad (2)$$

Where for the i^{th} largest trees, Dg_{LT} is the quadratic mean diameter, H_{LT} the mean height, and WD_{LT} the mean wood density averaged among the i^{th} largest trees.

Using a large database of forest inventories gathered across the Tropics (Figure 1), including secondary and old growth forest plots, we test the ability of the largest trees to provide information on various metrics estimated at 1-ha plot level, such as the mean quadratic diameter, the basal area (BA), the Lorey's height (i.e. plot-average height weighted by BA), the community wood density (i.e. plot-average wood density weighted by BA) and mean above-ground live biomass (AGB) (supplementary figure 1). While previous work focused on estimating biomass in Central African forests (Bastin *et al.*, 2015), the present study aims at generalizing the potential of large trees in predicting these different plot metrics at continental and pan-tropical scales. Taking advantage of a unique dataset gathered across the tropics (XX ha, YYY plots), we also investigate major differences in forest structure across the three main tropical regions, South America, Africa and South East Asia. We further discuss how this approach can be used to guide innovative RS techniques and increase the frequency and representativeness of ground data to support global calibration and validation of current and planned space missions. These include the NASA Global Ecosystem Dynamics Investigation (GEDI), NASA-ISRO Synthetic Aperture Radar (NISAR), and ESA P-band radar (BIOMASS). This study is a step forward in bringing together remote sensing and field sampling techniques for quantification of terrestrial C stocks in tropical forests.

Material & Methods

Database

For this study, we compiled standard forest inventories conducted in 867 1-hectare plots from 118 sites across the three tropical regions (Figure 1), including mature and secondary forests. Each site comprises all the plots in a given geographical location, i.e. within a 10 km radius and collected by a PI and its team. These consisted of 389 plots in America (69 sites), 302 plots in Africa (35 sites) and 176 plots in Asia (14 sites). Data were provided by Principal Investigators (see supplementary Table 1), and through datasets available at ForestPlots (https://www.forestplots.net/), TEAM (http://www.teamnetwork.org/) and CTFS (http://www.forestgeo.si.edu/) networks.

We selected plots located between 23°N and 23°S, including tropical islands, with an area of at least 1-ha to ensure stable intra-sample variance in basal area (Clark & Clark, 2000). Plots in which at least 90% of the stems were identified to species, and in which all stems with the diameter at 130 cm greater than or equal to 10 cm had been measured were included. Wood density, here recorded as the wood dry mass divided by its green volume, was assigned to each tree using the lowest available taxonomic level of botanical identifications (i.e. species or genus) and the corresponding average wood density recorded in the Global Wood Density Database (GWDD, Chave *et al.*, 2009; Zanne *et al.*, 2009). Botanical identification was harmonized through the Taxonomic Names Resolution Service (http://tnrs.iplantcollaborative.org), for both plot inventories and the GWDD. For trees not identified to species or genus (~5%), we used plot-average wood density. We estimated heights of all trees using Chave et al.'s (2014) pan-tropical diameter-height model which accounts for heterogeneity in the D-H relationship using an environmental proxy:

$$\ln(H) = 0.893 - E + 0.760 \ln(D) - 0.0340 \ln(D)^2 \quad (3)$$

Where D is the diameter at 130cm and E is a measure of environmental stress (Chave *et al.*, 2014). For sites with tree height measurements (N=20), we developed local D-H models, using a Michaelis-Menten function (Molto *et al.*, 2014). We used these local models to validate the

predicted Lorey's height (i.e. plot average height weighted by BA) from the largest trees, of which height has been estimated with a generic H-D model (equation 3, Chave et al. 2014). We estimated plot biomass as the sum of the biomass of live tree with diameter at 130 cm superior or equal to 10 cm, using the following pan-tropical allometric model (Réjou-Méchain *et al.*, 2017):

$$AGB=\exp(-2.024-0.896E+0.920\ln(WD)+2.795\ln(D)-0.0461(\ln(D^2))) \quad (4)$$

Plot-level metric estimation from the largest trees

The relationship between each plot metric, namely basal area (BA), the quadratic mean diameter (Dg), Lorey's height ($H_{BA;}$ the mean height weighted by the basal area) and the community wood density (WD_{BA}; the mean wood density weighted by the basal area), and those derived from largest trees was determined using an iterative procedure following Bastin et al. (2015). Trees were first ranked by decreasing diameter in each plot. An incremental procedure (i.e. including a new tree at each step) was used to sum or average information of the *i* largest trees for each plot metric. Specifically, each plot-level metric was predicted by the respective metric derived from the i^{th} largest trees. For each increment, the ability (goodness of fit) of the *i* largest trees to predict a given plot-metric was tested through a linear regression. To avoid overfitting, a Leave-One-Out procedure was used to develop independent site-specific models (N=118). Specifically, the model to be tested at a site was developed with data from all other sites. Errors were then estimated as the relative root mean square error (rRMSE) computed between observed and predicted values (X):

$$rRMSE = \bar{X} \sum \sqrt{\frac{(Xobs - Xpred)^2}{n}} \quad (5)$$

The form of the regression model (i.e. linear, exponential) was selected to ensure a normal distribution of the residuals.

To estimate plot basal area, we used a simple power-law constrained on the origin, as linear model resulted in non-normal residuals. Plot-level basal area (BA) was related to the basal area for the *i* largest trees (BA_i) using:

$$BA = b_1 \Sigma BA_i^{\gamma 1} \quad (6)$$

To estimate the quadratic mean diameter, Lorey's height and the wood density of the community, we used simple linear models relating the plot-level metrics and the value of the metrics for the *i* largest trees:

$$D_g = a_2 + b_2 D_{gi} \quad (7)$$

$$H_{BA} = a_3 + b_3 \overline{H_i} \quad (8)$$

$$WD_{BA} = a_4 + b_4 \overline{WD_i} \quad (9)$$

Both Lorey's height (H_{BA}) and the average height ($\overline{H_i}$) of the i^{th} largest trees depend on the same D-H allometry, which always contains uncertainty whether we use a local, a continental or a pan-tropical model. To test the dependence of the prediction of H_{BA} from $\overline{H_i}$ on the allometric model, we used measurement from Malebo in the Democratic Republic of the Congo, where all heights were measured on the ground (see supplementary figure 2).

The quality of the predictions of plot-level metrics from the largest trees is quantified using the relative root mean square error (rRMSE) between measured and predicted values, and displayed along the cumulated number of largest trees (Figure 2). Model coefficients are estimated for each metric derived from the largest trees (N_{LT}) and averaged across the 118 models (see supplementary table 2).

Mean rRMSE is plotted as a continuous variable, while its variation is presented as a continuous area between 5^{th} and the 95^{th} percentiles of observed rRMSE (Figure 2).

The optimal number of largest trees for plot-level biomass estimation

The optimal number of largest trees N_{LT} was determined from the prediction of each plot-level metric considered above, i.e. keeping a small number of trees while ensuring a low level of error for each structural parameter. We then predicted plot-level biomass from the N_{LT} model (equation 2). The final error was calculated by propagating the entire set of errors related to equation 4 (Réjou-Méchain *et al.*, 2017) in the N_{LT} model (i.e. error associated to each allometric model used). The model was then cross-validated across all plots (N=867).

Investigating residuals: what the largest trees do not explain

To understand the limits of predicting AGB through N_{LT}, we further investigated the relationship between AGB residuals and key structural and environmental variables using linear modelling. Forest structure was investigated through the total stem density (N), the quadratic mean diameter (Dg), Lorey's height (H_{BA}) and community wood density (WB_{BA}). As environmental data, we used the mean annual rainfall and the mean temperature computed over the last 10 years at each site using the Climate Research Unit data (New *et al.*, 1999, 2002), along with rough information on soil types (Carré. *et al.*, 2010). Major soil types were computed from the soil classification of the Harmonized World Soil Database into IPCC (intergovernmental panel on climate change) soil classes. In addition, considering observed differences in forest structure across tropical continents (Feldpausch *et al.*, 2011) and recent results on pan-tropical floristic affinities (Slik *et al.*, 2015), we tested for an effect of continent (America, Africa and Asia) on the AGB residuals.

The importance of each variable was evaluated by calculating the type II sum of squares that measures the decrease in residual sum of squares due to an added variable once all the other variables have been introduced into the model (Langsrud, 2003). Residuals were investigated at both plot and site levels, the latter analyzed to test for any influence of the diameter structure, which is usually unstable at the plot level due to the dominance of large trees on forest metrics at small scales (Clark & Clark, 2000). Here we use a principal component analysis (PCA) to summarize the information held in the diameter structure by ordinating the sites along the abundance of trees in each diameter class (from 10 to +100 cm by 10 cm bins).

Results

Plot-level metrics

Plot metrics averaged at the site level (867 plots, 118 sites) present important variations within and between continents. In our database, the quadratic mean diameter varies from 15 to 42 cm^2ha^{-1}, the basal area from 2 to 58 m^2ha-1, Lorey's height from 11 to 33 m and the wood density weighted by the basal area from 0.48 to 0.84 gcm^{-3} (Supplementary figure 1). Such important differences between minimal and maximal values are observed because our database cover sites with various forest types, from young forest colonizing savannas to old growth forest. However, most of our sites are found in mature forests, as shown by relatively high average and median value of each plot metric (average aboveground biomass = 302 $Mgha^{-1}$; supplementary figure 1). In general, highest values of aboveground biomass are found in Africa, driven by highest values of basal area and highest estimations of Lorey's height. Highest values of wood density weighted by basal area are found in America.

Plot-level estimation from the i largest trees

Overall, plot metrics at 1 ha scale were well predicted by the largest trees, with qualitative agreement among global and continental models (Figure 2).

When using the 20 largest trees to predict basal area (BA) and quadratic mean diameter (Dg), the mean rRMSE was < 16% and 12%, respectively (Figs 3a and 3b). Lorey's height (H_{BA}) and wood density weighted by basal area (WD_{BA}) were even better predicted (Figs 3c and 3d), with mean rRMSE of 4% for the 20 largest trees. The prediction of Lorey's height from the largest trees using local diameter-height model (supplementary Figure 2a) yielded results similar to those obtained using equation 3 of Chave et al. (2014). More importantly, it also yielded similar results to prediction of Lorey's height from the largest trees using plots where all the trees were measured on the ground (supplementary figure 2b). This suggests that our conclusions are robust to the uncertainty introduced by height-diameter allometric models.

AGB prediction from the largest trees

We selected “20” as the number of largest trees to predict plot metrics. The resulting model predicting AGB (Mg ha^{-1}) based on the 20 largest trees is:

$$AGB = 0.0735 \times (Dg_{20}H_{20}WD_{20})^{1.1332} \text{ (rRMSE=0.179; } R^2\text{=0.85; AIC= -260.18) (10)}$$

Because the exponent was close to 1, we also developed an alternative and more operationa l model with the exponent constrained to 1, given by:

$$AGB = 0.195 \times (Dg_{20}H_{20}WD_{20}) \text{ (rRMSE=0.177; } R^2\text{=0.85; AIC=-195) (11)}$$

Ground measurements of plot AGB were predicted by our N_{LT} model with the exponent constrained to 1, with a total error of 17.9% (Figure 4), a value which encompass the error of the N_{LT} model and the error related to the allometric model chosen. The Leave-One-Out cross-validation procedure yielded similar results (rRMSE=0.19; R^2=0.81), validating the use of the model on independent sites.

Determining the cause of residual variations

The explanatory variables all together explain about 37% of the variance in AGB both at plot and site levels when omitting the diameter structure, and about 63% at site level when included (Fig. 5). In general, forest structure and particularly the stem density explained most of the residuals (table 1; weights: 79% and 54% at plot- and site-level respectively). The stem density was followed by a continental effect (weights: 18%, 28% and 1%, respectively for Africa, South America and Asia) and by the effect of H_{BA} and WD_{BA} (respective weights: 1% and 0% at the plot level, 0% and 11% at the site level, and 23% and 0% when accounting for the diameter structure at the site level). Inclusion of the diameter structure provided the best explanation of residuals, with 63% of variance explained, and a weight of 69% for the first axis of the PCA (supplementary figure 3). This first axis of the PCA was related to the general abundance of trees at a site, and in particular medium-sized trees (40-60cm). Among environmental variables, only rainfall was significantly related to the residuals at the site level when the diameter structure was considered (2%).

Discussion

The largest trees, convergences and divergences between continents

Sampling a few largest trees per hectare generally allows an unbiased prediction of four key descriptors of forest structures across the Tropics. There is generally no improvement in predicting basal area, quadratic mean diameter, Lorey's height (H_{BA}) or community wood density beyond the first 10-to-20 largest trees (Figure 2, Figure 3a).In some cases, e.g. when a forest plot presents an abundant number of large trees (Figure 5d), increasing the number of trees sampled improves the model's accuracy. This is the case for BA for which rRMSE continues to decrease up to 100 largest trees (Figure 2a). In contrast, Lorey's height predictions are altered when a large number of trees are included (Figure 2c), i.e. when smaller, often suppressed, trees draw the average down (Farrior *et al.*, 2016). This might explain why the prediction of AGB does not mirror that of basal area (Figure 2b, Figure 3a), and suggest that the number of largest trees shall be set independently to each predictor considered. Interestingly, the evolution of relative error in AGB prediction as a function of the number of largest trees considered does not follow the same path between continents. For instance, the error of prediction saturates more quickly in Africa and Asia than Asia, where high variations of residuals are observed. Investigation of residuals showed that the diameter structure (Figure 5c, supplementary Figure 3b), and in particular the number of medium size trees (Figure 5d), drives variability in AGB predictions. It is therefore not surprising to see that in our dataset the site with higher levels of underestimations is the one with the highest number of medium size trees, which is found in Asia in the Western Ghats of India.

The good performance of models based on the 20 largest trees in predicting Lorey's height and community wood density at site level was not surprising. Both metrics were indeed weighted by basal area, driven *de facto* by the largest trees. Their consistency across sites and continents was not expected though. This suggests that the relationship between the 20 largest trees and descriptors of forest structures is stable across the tropics, and prove the generality of our approach. Slight differences are however noticeable when comparing the distribution of the pan-tropical model residuals across continents (Figure 6, supplementary

figure 4).In America, our pan-tropical model tend to slightly underestimate basal area (mean: -5%) and overestimate Lorey's height (mean: +3%) (supplementary figure 4), suggesting peculiar forest structures (i.e. higher tree height for a given diameter, and lower fractions of large trees, supplementary figure 2). In Asia, and in particular in Africa, large (i.e. DBH > 50 cm) trees are more abundant and encompass a large fraction of plot biomass. The basal area tends to be slightly overestimated in Africa, resulting in average to a 3% overestimation of AGB (Figure 6a).

Interestingly, while a recent global phylogenetic classification of tropical forest groups American with African forests vs. Asian forests (Slik *et al.*, 2018), our results tend more to single out American forests. Although this deserves further investigations, it might reveal a lack of close relationship between forest structure properties and phylogenic similarity, which echoes recent results on the absence of relationship between tropical forest diversity and biomass (Sullivan *et al.*, 2017).

Largest trees, a gateway to global monitoring of tropical forests

Revealing the predictive capacity held by the largest trees, our results constitute a major step forward to monitor forest structures and biomass stocks. The largest trees in tropical forests can therefore be used to accurately predict and efficiently infer various ground-measured properties (i.e. the quadratic mean diameter, the basal area, Lorey's height and community wood density), while previous work has predicted only biomass "estimates" (e.g. Slik *et al.*, 2013; Bastin *et al.*, 2015). This approach allows us to (i) describe forest structure independently of any biomass allometric model (ii) and cover local variations in D-H relationship, known to vary locally (Feldpausch *et al.*, 2011; Kearsley *et al.*, 2013;). It is also (iii) relatively insensitive to differences in floristic composition and community wood density (Poorter *et al.*, 2015).

Furthermore, the "largest trees" models were developed for each plot-level metric and for any number of largest trees. Thus, they do not rely on any arbitrary threshold of tree diameter. Note that the optimal number of largest trees to be measured (i.e. 20) was set for demonstration and can vary depending on the needs and capacities of each country or project (see supplementary table 2). In the same way, local models could integrate locally-developed

biomass models, when available. Consequently our approach (i) can be used in young or regenerating un-managed forests with a low “largest tree” diameter threshold and (ii) is compatible with recent remote sensing approaches able to single out canopy trees and describe their crown and height metrics (Ferraz *et al.*, 2016; Coomes *et al.*, 2017).

Aboveground biomass model from the largest trees, a multiple opportunity

Globally, the N_{LT} model for the 20 largest trees allows plot biomass to be predicted with 17.9% error. This result is a pan-tropical validation of results obtained in Central Africa (Bastin *et al.*, 2015). It opens new perspectives towards cost-effective methods to monitor forest structures and carbon stocks through largest trees metrics, i.e. metrics of objects directly intercepted by remote-sensing products.

Developing countries willing to implement a Reduction of Emissions from Deforestation and Forest Degradation (REDD+), shall also report on their carbon emissions (CE) and develop a national CE reference level (IPCC, 2006; Maniatis & Mollicone, 2010). However, most tropical countries lack capacities to assume multiple, exhaustive and costly forest carbon assessment (Romijn *et al.*, 2012). By measuring only a few large trees per hectare, our results show that it is possible to obtain unbiased estimates of aboveground C stocks in a time and cost-efficient manner. Assuming that 400 to 600 trees D > 10 cm are measured in a typical 1-ha sample plot, monitoring only 20 trees is a significant improvement. Although finding the 20 largest trees in a plot of several hundred individuals requires evaluating more than 20 trees, in practice, a conservative diameter threshold could be defined to ensure that the 20 largest trees are sampled. An alternative approach could also be found in the development of relascope-based approach adapted to detection of the largest trees in tropical forests. Using such approach would facilitate rapid field sampling in extensive areas to produce large scale AGB estimates. Those could fullfil the needs in calibration and validation of current and forthcoming space missions focused on aboveground biomass.

Our findings also points towards the potential effectiveness of using remote sensing techniques to characterize canopy trees. Here, remote sensing data could be used for direct measurement (e.g. tree level metrics such as height, crown width, crown height) of the largest

trees instead of indirect development of complex metrics (e.g. mean canopy height, texture) used to extrapolate forest properties. While some further refinements are needed, most of the tools required to develop “largest trees” models are readily available. In particular, Ferraz et al. (2016) developed an automated procedure to locate canopy trees based on airborne LiDAR data, to measure their height and crown area. Crown area could further be linked to basal area, as the logarithm of crown area is consistently correlated with a slope of 1.2-1.3 to the logarithm of tree diameter across the tropics (Blanchard *et al.*, 2016). Regarding wood density, hyperspectral signature offers a promising way to assess functional traits remotely (e.g. Asner *et al.*, 2017) which could potentially be tested to detect variability in wood properties. Alternative approaches could focus on the development of plot-level AGB prediction by replacing the basal area of the largest trees with their crown metrics. While the measurement of crown areas have yet to be generalized when inventorying plots, several biomass allometric models already partition trunk and crown mass (Jucker *et al.*, 2016; Ploton *et al.*, 2016; Coomes *et al.*, 2017).

The main limitation of our approach lies in the understory and sub-canopy trees. We show that most of the remaining variance is explained by variations in diameter structures, and in particular among the total stem density. Interestingly, stem density was generally identified as a poor predictor of plot biomass in tropical forests (Slik *et al.*, 2010; Lewis *et al.*, 2013). However, our results show that stem density explains most of the remaining variance (Table S1). This suggests that, in addition to trying to understand large-scale variations in large trees and other plot metrics, which can be directly quantified from remote sensing, we should also put more effort into understanding variation in smaller trees, which mainly drives total stem density and the total floristic diversity. Smaller trees are also essential to characterize forest dynamics and understand changes in carbon stocks. Several options are nonetheless possible from remote sensing, considering the variation in lidar point density below the canopy layer (D’Oliveira *et al.*, 2012), the distribution of leaf area density (Stark *et al.*, 2012, 2015; Tang & Dubayah, 2017) or the use of multitemporal lidar data to get information on forest gap

generation dynamics and consequently on forest diameter structure (Kellner *et al.*, 2009; Farrior *et al.*, 2016).

Large trees in degraded forests

If large trees are a key feature of unmanaged forests, they are conspicuously absent from managed or degraded forests. Indeed, large trees are targeted by selective or illegal logging, and are the first to disappear or to suffer from incidental damages when tropical forests are exploited for timber (Sist *et al.*, 2014). The loss of largest trees drastically changes forest structures and diameter distributions, and their loss is likely to counteract the consistency in forest structures observed through this study. Understanding how, or whether, managed forests deviate from our model predictions could help characterize forest degradation, which accounts for a large fraction of carbon loss worldwide (Baccini *et al.*, 2017), acknowledging that rapid post-disturbance biomass recovery (Rutishauser *et al.*, 2015) will remain hard to capture.

Conclusion – towards improved estimates of tropical forest biomass

The acquisition, accessibility and processing capabilities of very high spatial, spectral and temporal resolution remote sensing data has increases exponentially in recent years (Bastin *et al.*, 2017). However, to develop accurate global maps, we will have to obtain a greater number of field plots and develop new ways to use remote sensing data. Our results provide a step forward for both by (i) decreasing drastically the number of individual tree measurements required to get an accurate, yet less precise, estimate of plot biomass and (ii) opening the door to direct measurement of plot metrics measured from remote sensing to estimate plot biomass. As highlighted by Clark and Kellner (2012), new biomass allometric models relating plot-level biomass measured from destructive sampling and plot-level metric measured from remote-sensing products should be developed, as an alternative to current tree-level allometric models. Such an effort will lead largely to lower operational costs and uncertainties surrounding terrestrial C estimates, and consequently, will help developing countries in the development of national forest inventories and aid the scientific community in better understanding the effect of climate change on forest ecosystems.

Acknowledgments

J.-F.B. was supported for data collection by the FRIA (FNRS), ERAIFT (WBI), WWF and by the CoForTips project (ANR-12-EBID-0002); T.d.H. was supported by the COBIMFO project (Congo Basin integrated monitoring for forest carbon mitigation and biodiversity) funded by the Belgian Science Policy Office (Belspo); C.H.G was supported by the “Sud Expert Plantes” project of French Foreign Affairs, CIRAD and SCAC. Part of data in this paper was provided by the TEAM Network, the partnership between Conservation International, The Missouri Botanical Garden, The Smithsonian Institution and The Wildlife Conservation Society, and these institutions and the Gordon and Betty Moore Foundation. This is [number to be completed] publication of the technical series of the Biological Dynamics of Forest Fragment Project (INPA/STRI). We acknowledge data contributions from the TEAM network not listed as co-authors (upon voluntary basis). We thank Jean-Phillipe Puyravaud, Estação Científica Ferreira Penna (MPEG) and the Andrew Mellon Foundation and National Science Foundation (DEB 0742830). And finally, we thank Helen Muller-Landau for her careful revision and comments of the manuscript.

Contributions

J.F.Bastin and E.Rutishauser conceptualized the study, gathered the data, performed the analysis and wrote the manuscript. All the co-authors contributed by sharing data and reviewing the main text. A.R.Marshall, J.Poulsen and J.Kellner revised the English.

Conflict of interest

The authors declare there is no conflict of interest associated to this study.

Figures

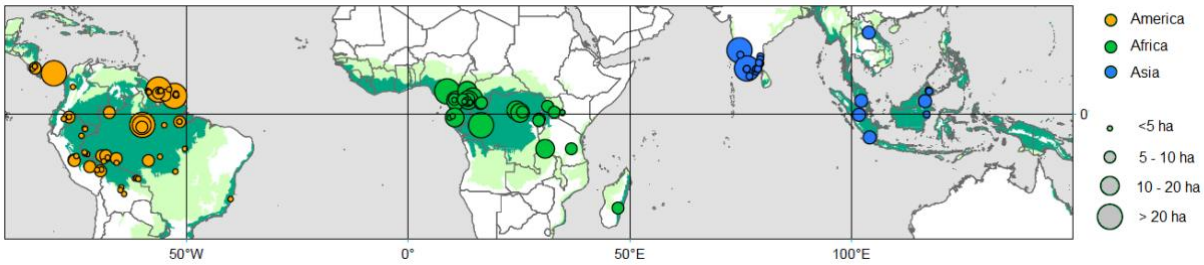

Figure 1. Geographic distribution of the plot database. We used 867 plots of 1 hectare from 118 sites. Dots are colored according to floristic affinities (Slik et al. 2015), with America, Africa and Asia respectively in orange, green and blue. They are also sized according the total area surveyed in each site.

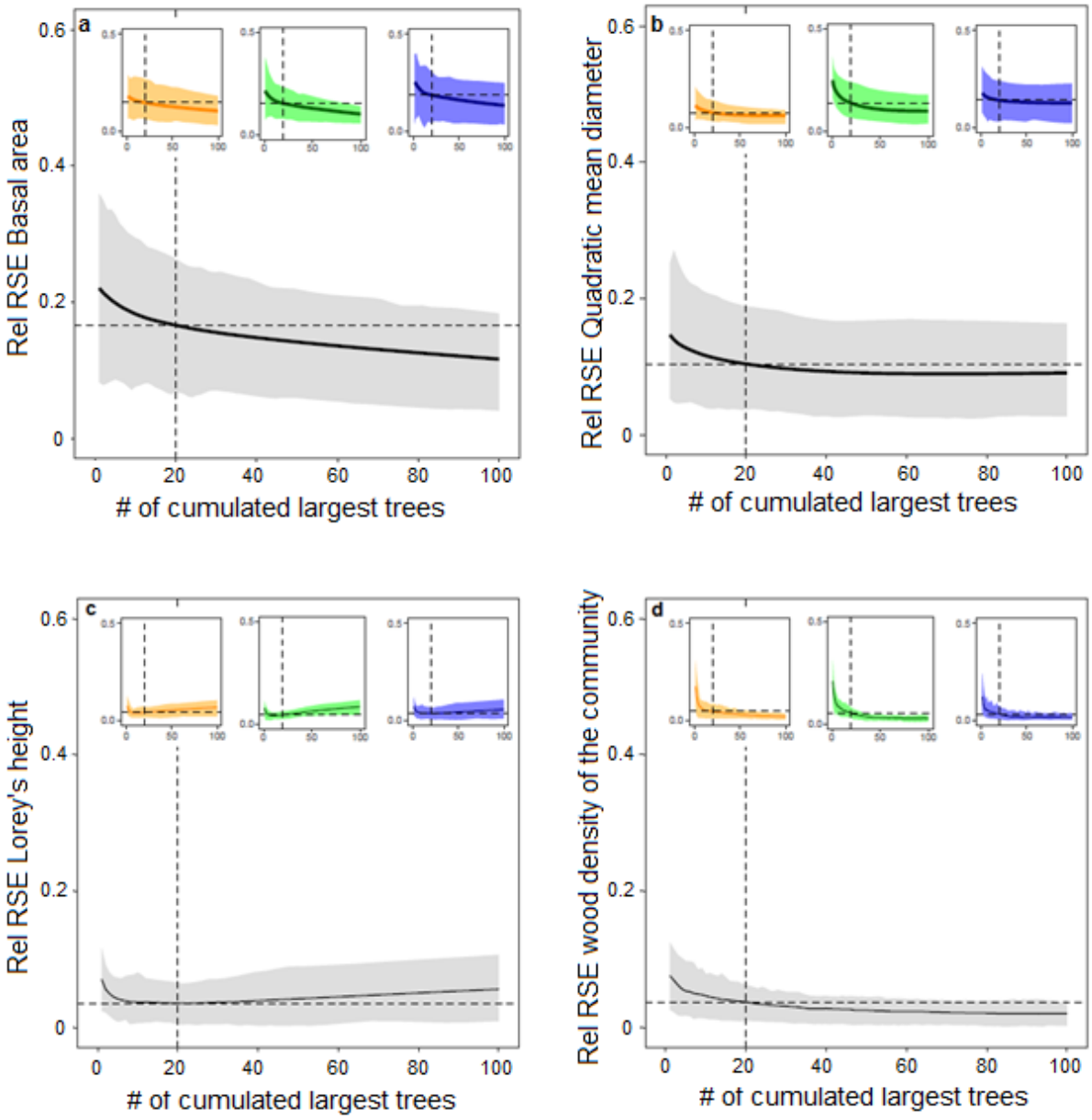

620

621 **Figure 2. Quality of the prediction of plot metrics from largest trees.** Variation of the
622 relative Root Mean Square Error (rRMSE) of the prediction of plot metric from i largest trees
623 versus the cumulative number of largest trees for (a) basal area, (b) quadratic mean diameter,
624 (c) Lorey's height and (d) wood density weighted by the basal area. Results are displayed at
625 the pan-tropical level (main plot in grey) and at the continental level (subplots; orange =
626 America; green = Africa; blue = Asia). The solid line and shading shows the mean rRMSE and
627 the 5th and the 95th percentiles. Dashed lines represent the mean rRMSE observed for each
628 model, when considering the 20 largest trees.

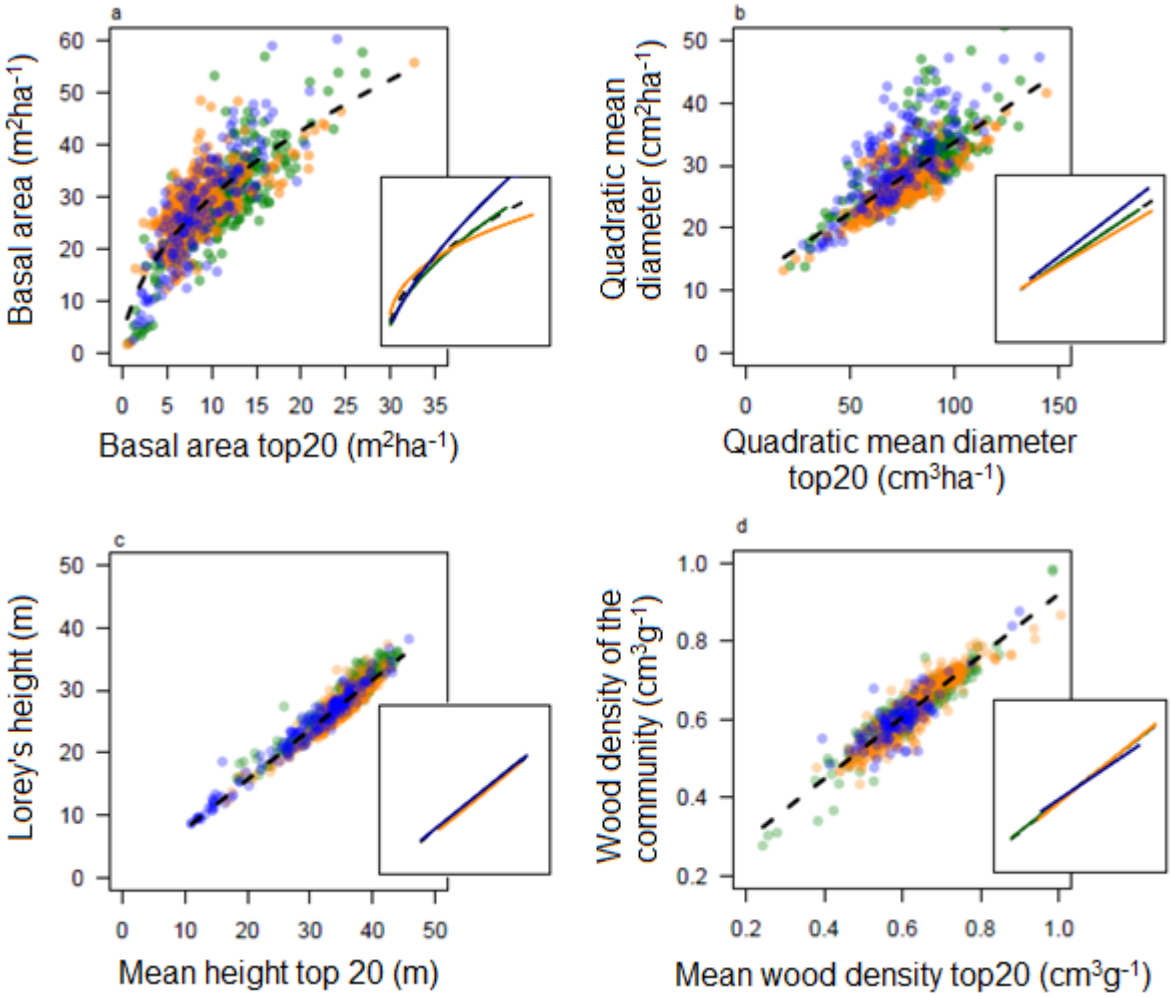

Figure 3. Prediction of plot metrics (y-axis) from the 20 largest trees (x-axis). Results are shown for (a) basal area, (b) quadratic mean diameter, (c) Lorey's Height and (d) wood density weighted by the basal area. Each dot corresponds to a single plot, colored in orange, green and blue for America, Africa and Asia respectively. Both pan-tropical (black dashed lines) and continental (coloured lines) regression models are displayed. These results show that substantial part of remaining variance, i.e. not explained by largest trees, is found when predicting the basal area and the quadratic mean diameter, with slight but significant differences between continents.

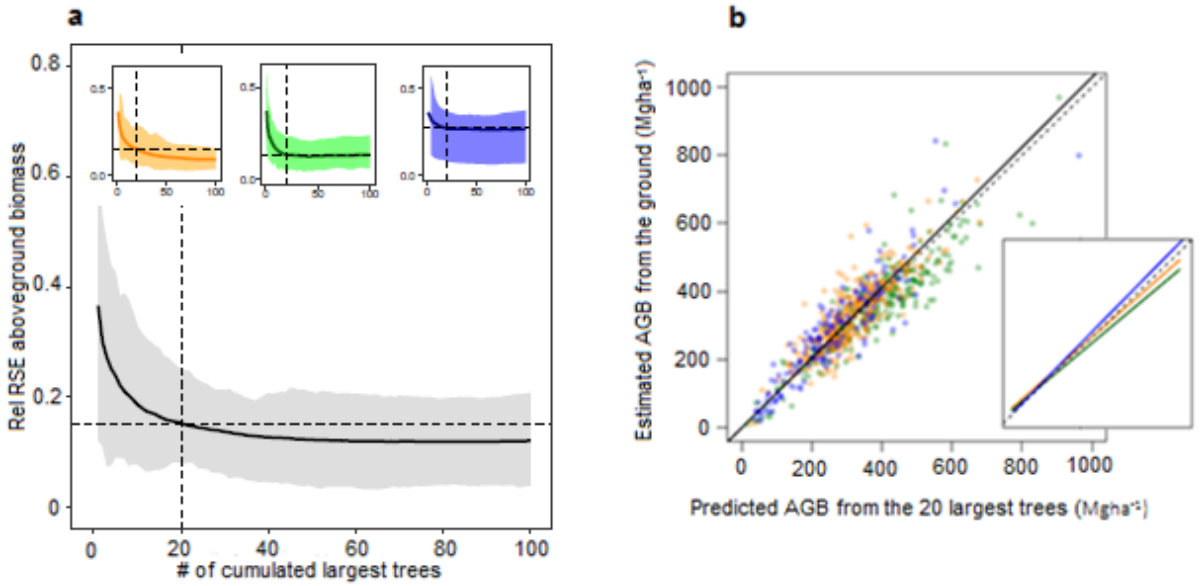

638

639 **Figure 4. Prediction of AGB from plot metrics of the 20 largest trees.** Results are shown
640 for the 867 plots, among the three continents colored orange, green and blue for America,
641 Africa and Asia respectively. The regression line of the model is shown as a continuous black
642 line while the dashed black line shows a 1:1 relationship. The figure shows an unbiased
643 prediction of AGB across the 867 plots, with slight but significant differences between the 3
644 continents.

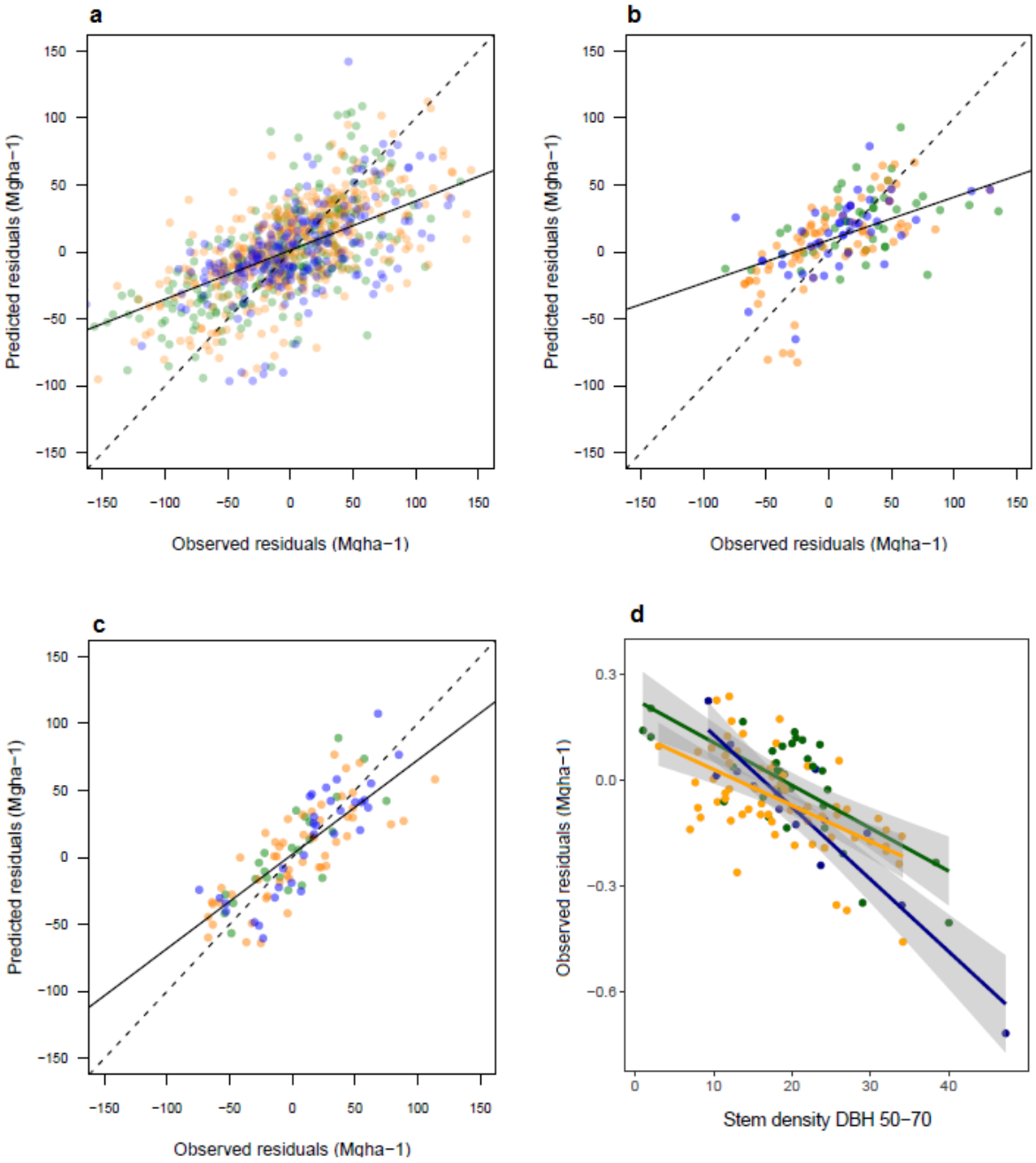

Figure 5. Predicted vs. observed residuals of above ground biomass predicted from the 20 largest trees. Residuals are explored at three different levels: (a) plot, (b) site [without considering the diameter structure as an explanatory variable], (c) site [considering the diameter structure] and (d) along the stem density of medium size trees. America, Africa and Asia are colored in orange, green and blue respectively. The figures show a good prediction of residuals in (a) and (b), driven by stem density, anda less biased prediction in (c), driven by

652 the diameter structure. Variance of observed residuals are also well explained by the stem
653 density of medium size trees (d), which mainly drive the first axis of the PCA.

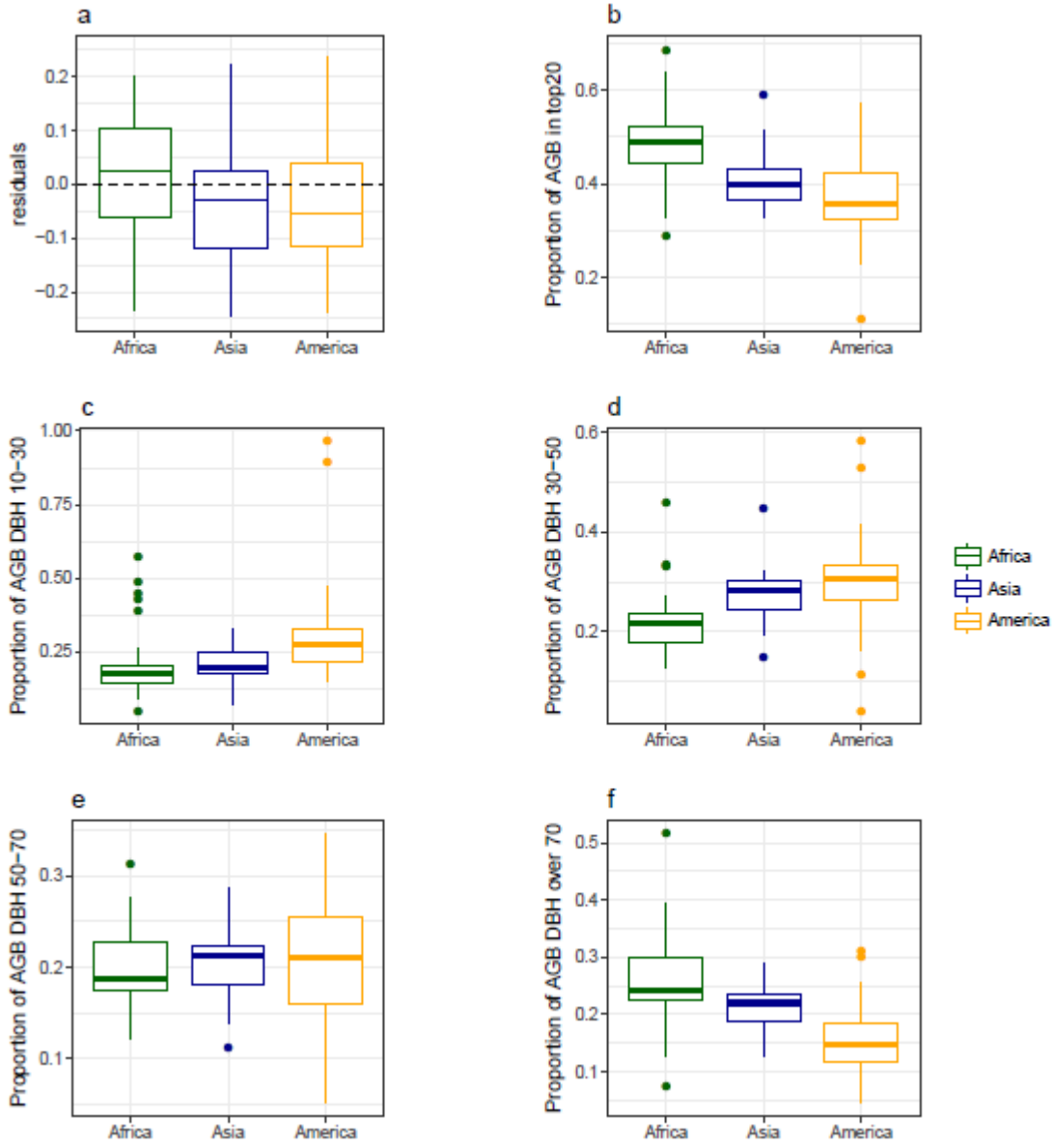

654

655 Figure 6. Comparison across continents of aboveground biomass prediction per site and their
656 contribution to different share of the diameter structure. Africa, Asia and America, are colored
657 in green, blue and orange, respectively. The distribution of the residuals of pan-tropical
658 aboveground biomass prediction from the 20 largest trees (a) shows predictions are slightly
659 overestimated in Africa (+2%), and slightly underestimated in Asia (-2%) and America (-6%).
660 The proportion of aboveground biomass in the 20 largest trees (b) is highest in Africa (48%),
661 followed by Asia (40%) and America (35%). The decomposition across four diameter classes
662 (c-f, i.e. from 10 to 30, 30 to 50, 50 to 70 and beyond 70 cm) of their relative share of the total
663 biomass shows that most of the biomass is found in the large trees in Africa, and in the small

664 to medium trees in America. Asia presenting a more balanced distribution of biomass across
665 the diameter structure.

666 **Tables**

667 **Table 1. Weight of each variable retained for the explanation of AGB residuals.** Weights
668 are calculated as a type ll sum of squares, which measures the decreased residual sum of
669 squares due to an added variable once all the other variables have been introduced into the
670 model. Results are shown for the exploration of residuals at the plot and at the site level, with
671 and without consideration of the diameter structure. Weights are dominated by structural
672 variables, and in particular the stem density and the diameter structure. Height, wood density
673 and continent have also a non-negligible influence on residuals.

Level of residual	Parameter	Weight	674
Plot			
	Stem density*	79	
	Continent*	18	
	Lorey's height*	1	
	Major soil types	1	
	Temperature	1	
	Wood density weighted by the basal area	0	
	Rainfall	0	
Site without diametric structure			
	Stem density*	54	
	Continent*	28	
	Wood density weighted by the basal area*	11	
	Rainfall	3	
	Major soil types	3	
	Temperature	2	
	Lorey's height	0	
Site with diametric structure			
	PCA axis 1*	69	
	Lorey's height*	23	
	Rainfall*	3	
	Major soil types	3	
	Continent	1	
	Temperature	1	
	Wood density weighted by the basal area	0	
	PCA axis 2	0	

675 **References**

676 Asner, G.G.P., Mascaro, J., Muller-Landau, H.H.C., Vieilledent, G., Vaudry, R., Rasamoelina,
677 M., Hall, J.S. & van Breugel, M. (2012) A universal airborne LiDAR approach for tropical
678 forest carbon mapping. *Oecologia*, **168**, 1147–1160.

679 Asner, G.P., Martin, R.E., Knapp, D.E., Tupayachi, R., Anderson, C.B., Sinca, F., Vaughn,
680 N.R. & Llactayo, W. (2017) Airborne laser-guided imaging spectroscopy to map forest
681 trait diversity and guide conservation. *Science*, **355**.

682 Asner, G.P. & Mascaro, J. (2014) Mapping tropical forest carbon: Calibrating plot estimates
683 to a simple LiDAR metric. *Remote Sensing of Environment*, **140**, 614–624.

684 Baccini, A., Walker, W., Carvalho, L., Farina, M., Sulla-Menashe, D. & Houghton, R.A. (2017)
685 Tropical forests are a net carbon source based on aboveground measurements of gain
686 and loss. *Science (New York, N.Y.)*, **358**, 230–234.

687 Barbier, N. & Couteron, P. (2015) Attenuating the bidirectional texture variation of satellite
688 images of tropical forest canopies. *Remote Sensing of Environment*, **171**, 245–260.

689 Barbier, N., Proisy, C., Véga, C., Sabatier, D. & Couteron, P. (2011) Bidirectional texture
690 function of high resolution optical images of tropical forest: An approach using LiDAR
691 hillshade simulations. *Remote Sensing of Environment*, **115**, 167–179.

692 Bastin, J.-F., Barbier, N., Couteron, P., Adams, B., Shapiro, A., Bogaert, J., De Cannière, C.,
693 De Canniére, C. & De Cannière, C. (2014) Aboveground biomass mapping of African
694 forest mosaics using canopy texture analysis: toward a regional approach. *Ecological*
695 *Applications*, **24**, 1984–2001.

696 Bastin, J.-F., Barbier, N., Réjou-Méchain, M., Fayolle, A., Gourlet-Fleury, S., Maniatis, D., De
697 Haulleville, T., Baya, F., Beeckman, H., Beina, D., Couteron, P., Chuyong, G., Dauby,
698 G., Doucet, J.-L., Droissart, V., Dufrêne, M., Ewango, C., Gillet, J.F., Gonmadje, C.H.,
699 Hart, T., Kavali, T., Kenfack, D., Libalah, M., Malhi, Y., Makana, J.-R., Pélissier, R.,
700 Ploton, P., Serckx, A., Sonké, B., Stevart, T., Thomas, D.W., De Cannière, C. &
701 Bogaert, J. (2015) Seeing Central African forests through their largest trees. *Scientific*
702 *Reports*, **5**.

703 Bastin, J.-F., Berrahmouni, N., Grainger, A., Maniatis, D., Mollicone, D., Moore, R., Patriarca,
704 C., Picard, N., Sparrow, B., Abraham, E.M., Aloui, K., Atesoglu, A., Attore, F., Bassüllü,
705 Ç., Bey, A., Garzuglia, M., García-Montero, L.G., Groot, N., Guerin, G., Laestadius, L.,
706 Lowe, A.J., Mamane, B., Marchi, G., Patterson, P., Rezende, M., Ricci, S., Salcedo, I.,
707 Diaz, A.S.-P., Stolle, F., Surappaeva, V. & Castro, R. (2017) The extent of forest in
708 dryland biomes. *Science*, **356**, 635–638.
709 Bennett, A.C., McDowell, N.G., Allen, C.D. & Anderson-Teixeira, K.J. (2015) Larger trees
710 suffer most during drought in forests worldwide. *Nature Plants*.
711 Blanchard, E., Birnbaum, P., Ibanez, T., Boutreux, T., Antin, C., Ploton, P., Vincent, G.,
712 Pouteau, R., Vandrot, H., Hequet, V., Barbier, N., Droissart, V., Sonké, B., Texier, N.,
713 Kamdem, N.G., Zebaze, D., Libalah, M. & Couteron, P. (2016) Contrasted allometries
714 between stem diameter, crown area, and tree height in five tropical biogeographic
715 areas. *Trees*, **30**, 1953–1968.
716 Carré., F., Hiederer, R., Blujdea, V. & Koeble, R. (2010) *Background Guide for the*
717 *Calculation of Land Carbon Stocks in the Biofuels Sustainability Scheme Drawing on*
718 *the 2006 IPCC Guidelines for National Greenhouse Gas Inventories. EUR 24573 EN.*,
719 Luxembourg.
720 Chave, J., Coomes, D., Jansen, S., Lewis, S.L., Swenson, N.G. & Zanne, A.E. (2009)
721 Towards a worldwide wood economics spectrum. *Ecology letters*, **12**, 351–66.
722 Chave, J., Réjou-Méchain, M., Búrquez, A., Chidumayo, E., Colgan, M.S., Delitti, W.B.C.,
723 Duque, A., Eid, T., Fearnside, P.M., Goodman, R.C., Henry, M., Martínez-Yrízar, A.,
724 Mugasha, W.A., Muller-Landau, H.C., Mencuccini, M., Nelson, B.W., Ngomanda, A.,
725 Nogueira, E.M., Ortiz-Malavassi, E., Pélissier, R., Ploton, P., Ryan, C.M., Saldarriaga,
726 J.G. & Vieilledent, G. (2014) Improved allometric models to estimate the aboveground
727 biomass of tropical trees. *Global change biology*, **20**, 3177–3190.
728 Chave, J., Riera, B., Dubois, M.-A. & Riéra, B. (2001) Estimation of biomass in a neotropical
729 forest of French Guiana : spatial and temporal variability. *Journal of Tropical Ecology*,
730 **17**, 79–96.

731 Clark, D.B. & Clark, D.A. (1996) Abundance, growth and mortality of very large trees in
732 neotropical lowland rain forest. *Forest Ecology and Management*, **80**, 235–244.
733 Clark, D.B. & Clark, D.A. (2000) Landscape-scale variation in forest structure and biomass in
734 a tropical rain forest. *Forest Ecology and Management*, **137**, 185–198.
735 Clark, D.B. & Kellner, J.R. (2012) Tropical forest biomass estimation and the fallacy of
736 misplaced concreteness. *Journal of Vegetation Science*, **23**, 1191–1196.
737 Coomes, D.A., Dalponte, M., Jucker, T., Asner, G.P., Banin, L.F., Burslem, D.F.R.P., Lewis,
738 S.L., Nilus, R., Phillips, O.L., Phua, M.-H. & Qie, L. (2017) Area-based vs tree-centric
739 approaches to mapping forest carbon in Southeast Asian forests from airborne laser
740 scanning data. *Remote Sensing of Environment*, **194**, 77–88.
741 D'Oliveira, M.V.N., Reutebuch, S.E., McGaughey, R.J. & Andersen, H.-E. (2012) Estimating
742 forest biomass and identifying low-intensity logging areas using airborne scanning lidar
743 in Antimary State Forest, Acre State, Western Brazilian Amazon. *Remote Sensing of*
744 *Environment*, **124**, 479–491.
745 Farrior, C.E., Bohlman, S.A., Hubbell, S. & Pacala, S.W. (2016) Dominance of the
746 suppressed: Power-law size structure in tropical forests. *Science*, **351**.
747 Fayolle, A., Loubota Panzou, G.J., Drouet, T., Swaine, M.D., Bauwens, S., Vleminckx, J.,
748 Biwole, A., Lejeune, P. & Doucet, J.-L. (2016) Taller trees, denser stands and greater
749 biomass in semi-deciduous than in evergreen lowland central African forests. *Forest*
750 *Ecology and Management*, **374**, 42–50.
751 Feldpausch, T.R., Banin, L., Phillips, O.L., Baker, T.R., Lewis, S.L., Quesada, C. a., Affum-
752 Baffoe, K., Arets, E.J.M.M., Berry, N.J., Bird, M., Brondizio, E.S., de Camargo, P.,
753 Chave, J., Djagbletey, G., Domingues, T.F., Drescher, M., Fearnside, P.M., França,
754 M.B., Fyllas, N.M., Lopez-Gonzalez, G., Hladik, a., Higuchi, N., Hunter, M.O., Iida, Y.,
755 Salim, K. a., Kassim, a. R., Keller, M., Kemp, J., King, D. a., Lovett, J.C., Marimon,
756 B.S., Marimon-Junior, B.H., Lenza, E., Marshall, a. R., Metcalfe, D.J., Mitchard, E.T. a.,
757 Moran, E.F., Nelson, B.W., Nilus, R., Nogueira, E.M., Palace, M., Patiño, S., Peh, K.S.-
758 H., Raventos, M.T., Reitsma, J.M., Saiz, G., Schrodt, F., Sonké, B., Taedoumg, H.E.,

759 Tan, S., White, L., Wöll, H. & Lloyd, J. (2011) Height-diameter allometry of tropical forest
760 trees. *Biogeosciences*, **8**, 1081–1106.
761 Feldpausch, T.R., Lloyd, J., Lewis, S.L., Brienen, R.J.W., Gloor, E., Monteagudo Mendoza,
762 a., Lopez-Gonzalez, G., Banin, L., Abu Salim, K., Affum-Baffoe, K., Alexiades, M.,
763 Almeida, S., Amaral, I., Andrade, a., Aragão, L.E.O.C., Araujo Murakami, a., Arets,
764 E.J.M.M., Arroyo, L., Baker, T.R., Bánki, O.S., Berry, N.J., Cardozo, N., Chave, J.,
765 Comiskey, J. a., Dávila, E. a., de Oliveira, a., DiFiore, a., Djagbletey, G., Domingues,
766 T.F., Erwin, T.L., Fearnside, P.M., França, M.B., Freitas, M. a., Higuchi, N., Iida, Y.,
767 Jiménez, E., Kassim, a. R., Killeen, T.J., Laurance, W.F., Lovett, J.C., Malhi, Y.,
768 Marimon, B.S., Marimon-Junior, B.H., Lenza, E., Marshall, a. R., Mendoza, C.,
769 Metcalfe, D.J., Mitchard, E.T. a., Nelson, B.W., Nilus, R., Nogueira, E.M., Parada, a.,
770 Peh, K.S.-H., Pena Cruz, a., Peñuela, M.C., Pitman, N.C. a., Prieto, a., Quesada, C.
771 a., Ramírez, F., Ramírez-Angulo, H., Reitsma, J.M., Rudas, a., Saiz, G., Salomão,
772 R.P., Schwarz, M., Silva, N., Silva-Espejo, J.E., Silveira, M., Sonké, B., Stropp, J.,
773 Taedoumg, H.E., Tan, S., ter Steege, H., Terborgh, J., Torello-Raventos, M., van der
774 Heijden, G.M.F., Vásquez, R., Vilanova, E., Vos, V., White, L., Wilcock, S., Woell, H. &
775 Phillips, O.L. (2012) Tree height integrated into pan-tropical forest biomass estimates.
776 *Biogeosciences Discussions*, **9**, 2567–2622.
777 Ferraz, A., Saatchi, S., Mallet, C. & Meyer, V. (2016) Lidar detection of individual tree size in
778 tropical forests. *Remote Sensing of Environment*, **183**, 318–333.
779 Gibbs, H.K., Brown, S., Niles, J.O. & Foley, J. a (2007) Monitoring and estimating tropical
780 forest carbon stocks: making REDD a reality. *Environmental Research Letters*, **2**, 1–13.
781 Harms, K.E., Wright, S.J., Calderón, O., Hernández, a & Herre, E. a (2000) Pervasive
782 density-dependent recruitment enhances seedling diversity in a tropical forest. *Nature*,
783 **404**, 493–5.
784 Ho Tong Minh, D., Le Toan, T., Rocca, F., Tebaldini, S., Villard, L., Réjou-Méchain, M.,
785 Phillips, O.L., Feldpausch, T.R., Dubois-Fernandez, P., Scipal, K. & Chave, J. (2016)
786 SAR tomography for the retrieval of forest biomass and height: Cross-validation at two

787 tropical forest sites in French Guiana. *Remote Sensing of Environment*, **175**, 138–147.
788 IPCC (2006) *2006 IPCC Guidelines for National Greenhouse Gas Inventories, Prepared by*
789 *the National Greenhouse Gas Inventories Programme*, IGES. (ed. by H.S. Eggleston),
790 L. Buendia), K. Miwa), T. Ngara), and K. Tanabe) Japan, Japan.
791 Jucker, T., Caspersen, J., Chave, J., Antin, C., Barbier, N., Bongers, F., Dalponte, M., van
792 Ewijk, K.Y., Forrester, D.I., Haeni, M., Higgins, S.I., Holdaway, R.J., Iida, Y., Lorimer, C.,
793 Marshall, P.L., Momo, S., Moncrieff, G.R., Ploton, P., Poorter, L., Rahman, K.A.,
794 Schlund, M., Sonké, B., Sterck, F.J., Trugman, A.T., Usoltsev, V.A., Vanderwel, M.C.,
795 Waldner, P., Wedeux, B.M.M., Wirth, C., Wöll, H., Woods, M., Xiang, W., Zimmermann,
796 N.E. & Coomes, D.A. (2016) Allometric equations for integrating remote sensing
797 imagery into forest monitoring programmes. *Global Change Biology*, n/a-n/a.
798 Kearsley, E., de Haulleville, T., Hufkens, K., Kidimbu, A., Toirambe, B., Baert, G., Huygens,
799 D., Kebede, Y., Defourny, P., Bogaert, J., Beeckman, H., Steppe, K., Boeckx, P. &
800 Verbeeck, H. (2013) Conventional tree height-diameter relationships significantly
801 overestimate aboveground carbon stocks in the Congo Basin. *Nature communications*.
802 Kellner, J.R., Clark, D.B. & Hubbell, S.P. (2009) Pervasive canopy dynamics produce short-
803 term stability in a tropical rain forest landscape. *Ecology Letters*, **12**, 155–164.
804 Kellner, J.R. & Hubbell, S.P. (2017) Adult mortality in a low-density tree population using
805 high-resolution remote sensing. *Ecology*, **98**, 1700–1709.
806 Langsrud, Ø. (2003) ANOVA for unbalanced data: Use Type II instead of Type III sums of
807 squares. *Statistics and Computing*, **13**, 163–167.
808 Laurance, W.F., Delamônica, P., Laurance, S.G., Vasconcelos, H.L. & Lovejoy, T.E. (2000)
809 Conservation: Rainforest fragmentation kills big trees. *Nature*, **404**, 836–836.
810 Lewis, S.L.L., Sonké, B., Sunderland, T., Begne, S.K.S.K., Lopez-Gonzalez, G., Heijden,
811 G.M.F. Van Der, Phillips, O.L.O.L., Affum-Baffoe, K., Baker, T.R.T.R., Banin, L., Bastin,
812 J.-F.J.-F., Beeckman, H., Boeckx, P., Bogaert, J., De Cannière, C., Chezeaux, V., Clark,
813 C.J.C.J., Collins, M., Djagbletey, G., Droissart, V., Doucet, J.-L.J.-L., Ewango,
814 C.E.N.C.E.N., Fauset, S., Feldpausch, T.R.R., Foli, E.G., Gillet, J.-F.J.-F., Hamilton,

A.C.A.C., Harris, D.J.D.J., Hart, T.B.T.B., de Haulleville, T., Hladik, A., Hufkens, K., Huygens, D., Jeanmart, P., Jeffery, K.J., Kamdem, M.-N.D., Kearlsey, E., Leal, M.E.E., Lloyd, J., Lovett, J.C.J.C., Makana, J.-R.J.-R., Malhi, Y., Marshall, A.R.R., Ojo, L., Peh, K.S.-H.K.S.-H., Pickavance, G., Poulsen, J.R., Reitsma, M., Sheil, D., Simo, M., Steppe, K., Taedoumg, H.E.E., Talbot, J., Taplin, J.J.R.D., Taylor, D., Thomas, S.C.S.C., Toirambe, B., Verbeeck, H., Vleminckx, J., White, L.J.T.J.T., Willcock, S., Woell, H., Zemagho, L., van der Heijden, G.M.F., Phillips, O.L.O.L., Affum-Baffoe, K., Baker, T.R.T.R., Banin, L., Bastin, J.-F.J.-F., Beeckman, H., Boeckx, P., Bogaert, J., De Cannière, C., Chezeaux, E., Clark, C.J.C.J., Collins, M., Djagbletey, G., Djuikouo, M.N.K., Droissart, V., Doucet, J.-L.J.-L., Ewango, C.E.N.C.E.N., Fauset, S., Feldpausch, T.R.R., Foli, E.G., Gillet, J.-F.J.-F., Hamilton, A.C.A.C., Harris, D.J.D.J., Hart, T.B.T.B., de Haulleville, T., Hladik, A., Hufkens, K., Huygens, D., Jeanmart, P., Jeffery, K.J., Kearsley, E., Leal, M.E.E., Lloyd, J., Lovett, J.C.J.C., Makana, J.-R.J.-R., Malhi, Y., Marshall, A.R.R., Ojo, L., Peh, K.S.-H.K.S.-H., Pickavance, G., Poulsen, J.R., Reitsma, J.M., Sheil, D., Simo, M., Steppe, K., Taedoumg, H.E.E., Talbot, J., Taplin, J.J.R.D., Taylor, D., Thomas, S.C.S.C., Toirambe, B., Verbeeck, H., Vleminckx, J., White, L.J.T.J.T., Willcock, S., Woell, H. & Zemagho, L. (2013) Above-ground biomass and structure of 260 African tropical forests. *Philosophical transactions of the Royal Society of London. Series B, Biological sciences*, **368**.

Lindenmayer, D.B., Laurance, W.F. & Franklin, J.F. (2012) Global decline in large old trees. *Science*, **338**, 1305–1306.

Malhi, Y., Wood, D., Baker, T.R., Wright, J., Phillips, O.L., Cochrane, T., Meir, P., Chave, J., Almeida, S., Arroyo, L., Higuchi, N., Killeen, T.J., Laurance, S.G., Laurance, W.F., Lewis, S.L., Monteagudo, A., Neill, D. a., Vargas, P.N., Pitman, N.C. a., Quesada, C.A., Salomao, R., Silva, J.N.M., Lezama, A.T., Terborgh, J., Martinez, R.V. & Vinceti, B. (2006) The regional variation of aboveground live biomass in old-growth Amazonian forests. *Global Change Biology*, **12**, 1107–1138.

Maniatis, D. & Mollicone, D. (2010) Options for sampling and stratification for national forest

inventories to implement REDD+ under the UNFCCC. *Carbon balance and management*, **5**, 9.

Mascaro, J., Detto, M., Asner, G.P. & Muller-Landau, H.C. (2011) Evaluating uncertainty in mapping forest carbon with airborne LiDAR. *Remote Sensing of Environment*, **115**, 3770–3774.

Meakem, V., Tepley, A.J., Gonzalez-Akre, E.B., Herrmann, V., Muller-Landau, H.C., Wright, S.J., Hubbell, S.P., Condit, R. & Anderson-Teixeira, K.J. (2017) Role of tree size in moist tropical forest carbon cycling and water deficit responses. *New Phytologist*.

Molto, Q., Hérault, B., Boreux, J.-J., Daullet, M., Rousteau, A. & Rossi, V. (2014) Predicting tree heights for biomass estimates in tropical forests – a test from French Guiana. *Biogeosciences*, **11**, 3121–3130.

Nepstad, D.C., Tohver, I.M., Ray, D., Moutinho, P. & Cardinot, G. (2007) Mortality of large trees and lianas following experimental drought in an Amazon forest. *Ecology*, **88**, 2259–69.

New, M., Hulme, M., Jones, P., New, M., Hulme, M. & Jones, P. (1999) Representing Twentieth-Century Space–Time Climate Variability. Part I: Development of a 1961–90 Mean Monthly Terrestrial Climatology. *Journal of Climate*, **12**, 829–856.

New, M., Lister, D., Hulme, M. & Makin, I. (2002) A high-resolution data set of surface climate over global land areas. *Climate Research*, **21**, 1–25.

Ploton, P., Barbier, N., Couteron, P., Antin, C.M., Ayyappan, N., Balachandran, N., Barathan, N., Bastin, J.-F., Chuyong, G., Dauby, G., Droissart, V., Gastellu-Etchegorry, J.-P., Kamdem, N.G., Kenfack, D., Libalah, M., Mofack, G., Momo, S.T., Pargal, S., Petronelli, P., Proisy, C., Réjou-Méchain, M., Sonké, B., Texier, N., Thomas, D., Verley, P., Zebaze Dongmo, D., Berger, U. & Pélissier, R. (2017) Toward a general tropical forest biomass prediction model from very high resolution optical satellite images. *Remote Sensing of Environment*, **200**.

Ploton, P., Barbier, N., Takoudjou Momo, S., Réjou-Méchain, M., Boyemba Bosela, F., Chuyong, G., Dauby, G., Droissart, V., Fayolle, A., Goodman, R.C., Henry, M.,

871 Kamdem, N.G., Mukirania, J.K., Kenfack, D., Libalah, M., Ngomanda, A., Rossi, V.,
872 Sonké, B., Texier, N., Thomas, D., Zebaze, D., Couteron, P., Berger, U. & Pélissier, R.
873 (2016) Closing a gap in tropical forest biomass estimation: taking crown mass variation
874 into account in pantropical allometries. *Biogeosciences*, **13**, 1571–1585.
875 Ploton, P., Pélissier, R. & Proisy, C. (2012) Assessing aboveground tropical forest biomass
876 using Google Earth canopy images. *Ecological Applications*, **22**, 993–1003.
877 Poorter, L., van der Sande, M.T., Thompson, J., Arets, E.J.M.M., Alarcón, A., Álvarez-
878 Sánchez, J., Ascarrunz, N., Balvanera, P., Barajas-Guzmán, G., Boit, A., Bongers, F.,
879 Carvalho, F.A., Casanoves, F., Cornejo-Tenorio, G., Costa, F.R.C., de Castilho, C. V.,
880 Duivenvoorden, J.F., Dutrieux, L.P., Enquist, B.J., Fernández-Méndez, F., Finegan, B.,
881 Gormley, L.H.L., Healey, J.R., Hoosbeek, M.R., Ibarra-Manríquez, G., Junqueira, A.B.,
882 Levis, C., Licona, J.C., Lisboa, L.S., Magnusson, W.E., Martínez-Ramos, M., Martínez-
883 Yrizar, A., Martorano, L.G., Maskell, L.C., Mazzei, L., Meave, J.A., Mora, F., Muñoz, R.,
884 Nytch, C., Pansonato, M.P., Parr, T.W., Paz, H., Pérez-García, E.A., Rentería, L.Y.,
885 Rodríguez-Velazquez, J., Rozendaal, D.M.A., Ruschel, A.R., Sakschewski, B., Salgado-
886 Negret, B., Schietti, J., Simões, M., Sinclair, F.L., Souza, P.F., Souza, F.C., Stropp, J.,
887 ter Steege, H., Swenson, N.G., Thonicke, K., Toledo, M., Uriarte, M., van der Hout, P.,
888 Walker, P., Zamora, N. & Peña-Claros, M. (2015) Diversity enhances carbon storage in
889 tropical forests. *Global Ecology and Biogeography*, **24**, 1314–1328.
890 Proisy, C., Couteron, P. & Fromard, F. (2007) Predicting and mapping mangrove biomass
891 from canopy grain analysis using Fourier-based textural ordination of IKONOS images.
892 *Remote Sensing of Environment*, **109**, 379–392.
893 Réjou-Méchain, M., Tanguy, A., Piponiot, C., Chave, J. & Hérault, B. (2017) biomass : an r
894 package for estimating above-ground biomass and its uncertainty in tropical forests.
895 *Methods in Ecology and Evolution*, **8**, 1163–1167.
896 Remm, J. & Lõhmus, A. (2011) Tree cavities in forests – The broad distribution pattern of a
897 keystone structure for biodiversity. *Forest Ecology and Management*, **262**, 579–585.
898 Romijn, E., Herold, M., Kooistra, L., Murdiyarso, D. & Verchot, L. (2012) Assessing

capacities of non-Annex I countries for national forest monitoring in the context of REDD+. *Environmental Science & Policy*, **19**–**20**, 33–48.

Rutishauser, E., Hérault, B., Baraloto, C., Blanc, L., Descroix, L., Sotta, E.D., Ferreira, J., Kanashiro, M., Mazzei, L., d'Oliveira, M.V.N., de Oliveira, L.C., Peña-Claros, M., Putz, F.E., Ruschel, A.R., Rodney, K., Roopsind, A., Shenkin, A., da Silva, K.E., de Souza, C.R., Toledo, M., Vidal, E., West, T.A.P., Wortel, V. & Sist, P. (2015) Rapid tree carbon stock recovery in managed Amazonian forests. *Current biology : CB*, **25**, R787-8.

Rutishauser, E., Wagner, F., Herault, B., Nicolini, E.-A. & Blanc, L. (2010) Contrasting above-ground biomass balance in a Neotropical rain forest. *Journal of Vegetation Science*, 672–682.

Saatchi, S.S., Houghton, R. a., Dos Santos Alvalá, R.C., Soares, J. V. & Yu, Y. (2007) Distribution of aboveground live biomass in the Amazon basin. *Global Change Biology*, **13**, 816–837.

Sist, P., Mazzei, L., Blanc, L. & Rutishauser, E. (2014) Large trees as key elements of carbon storage and dynamics after selective logging in the Eastern Amazon. *Forest Ecology and Management*, **318**, 103–109.

Slik, J.W.F., Aiba, S.-I., Brearley, F.Q., Cannon, C.H., Forshed, O., Kitayama, K., Nagamasu, H., Nilus, R., Payne, J., Paoli, G., Poulsen, A.D., Raes, N., Sheil, D., Sidiyasa, K., Suzuki, E. & Van Valkenburg, J.L.C.H. (2010) Environmental correlates of tree biomass, basal area, wood specific gravity and stem density gradients in Borneo's tropical forests. *Global Ecology and Biogeography*, **19**, 50–60.

Slik, J.W.F., Alvarez-loayza, P., Alves, L.F., Ashton, P., Balvanera, P., Bastian, M.L., Bellingham, P.J., Berg, E. Van Den, Bernacci, L., Conceição, P., Blanc, L., Böhning-gaese, K., Boeckx, P., Boyle, B., Bradford, M., Brearley, F.Q., Hockemba, B., Bunyavejchewin, S., Matos, C.L., Castillo-santiago, M., Eduardo, L.M., Chai, S., Chen, Y., Colwell, R.K., Robin, C.L., Clark, C., Clark, D.B., Deborah, A., Culmsee, H., Damas, K., Dattaraja, H.S., Dauby, G., Davidar, P., Dewalt, S.J., Doucet, J., Duque, A., Durigan, G., Eichhorn, K.A.O., Pedro, V., Eler, E., Ewango, C., Farwig, N., Feeley, K.J., Ferreira,

L., Field, R., Ary, T., Filho, D.O., Fletcher, C., Forshed, O., Fredriksson, G., Gillespie, T., Amarnath, G., Griffith, D.M., Grogan, J., Gunatilleke, N., Harris, D., Harrison, R., Hector, A., Homeier, J., Imai, N., Itoh, A., Jansen, P.A., Joly, C.A., Jong, B.H.J. De, Kartawinata, K., Kearsley, E., Kelly, D.L., Kenfack, D., Kitayama, K., Kooyman, R., Larney, E., Laurance, S., Laurance, W.F., Michael, J., Leao, I., Letcher, S.G., Lindsell, J., Lu, X., Mansor, A., Marjokorpi, A., Martin, E.H., Meilby, H., Melo, F.P.L., Metcalfe, D.J., Vincent, P., Metzger, J.P., Millet, J., Mohandass, D., Juan, C., Nagamasu, H., Nilus, R., Ochoa-gaona, S., Paudel, E., Permana, A., Maria, T.F., Rovero, F., Rozak, A.H., Santos, B.A., Santos, F., Sarker, S.K., Satdichanh, M., Schmitt, C.B., Schöngart, J., Tabarelli, M., Tang, J., Targhetta, N., Theilade, I., Thomas, D.W., Tchouto, P., Hurtado, J., Valkenburg, J.L.C.H. Van, Do, T. Van, Verbeeck, H., Adekunle, V., Vieira, S.A., Alvarez-loayza, P., Alves, L.F., Berg, E. Van Den & Bernacci, L. (2015) An estimate of the number of tropical tree species. *Proceedings of the National Academy of Sciences*, **112**, E4628–E4629.

Slik, J.W.F., Franklin, J., Arroyo-Rodríguez, V., Field, R., Aguilar, S., Aguirre, N., Ahumada, J., Aiba, S.-I., Alves, L.F., Anitha, K., Avella, A., Mora, F., Aymard, G.A.C., Báez, S., Balvanera, P., Bastian, M.L., Bastin, J.-F., Bellingham, P.J., Van Den Berg, E., Da Conceição Bispo, P., Boeckx, P., Boehning-Gaese, K., Bongers, F., Boyle, B., Brambach, F., Brearley, F.Q., Brown, S., Chai, S.-L., Chazdon, R.L., Chen, S., Chhang, P., Chuyong, G., Ewango, C., Coronado, I.M., Cristóbal-Azkarate, J., Culmsee, H., Damas, K., Dattaraja, H.S., Davidar, P., DeWalt, S.J., DIn, H., Drake, D.R., Duque, A., Durigan, G., Eichhorn, K., Eler, E.S., Enoki, T., Ensslin, A., Fandohan, A.B., Farwig, N., Feeley, K.J., Fischer, M., Forshed, O., Garcia, Q.S., Garkoti, S.C., Gillespie, T.W., Gillet, J.-F., Gonmadje, C., Granzow-De La Cerda, I., Griffith, D.M., Grogan, J., Hakeem, K.R., Harris, D.J., Harrison, R.D., Hector, A., Hemp, A., Homeier, J., Hussain, M.S., Ibarra-Manríquez, G., Hanum, I.F., Imai, N., Jansen, P.A., Joly, C.A., Joseph, S., Kartawinata, K., Kearsley, E., Kelly, D.L., Kessler, M., Killeen, T.J., Kooyman, R.M., Laumonier, Y., Laurance, S.G., Laurance, W.F., Lawes, M.J., Letcher, S.G., Lindsell, J.,

955 Lovett, J., Lozada, J., Lu, X., Lykke, A.M., Bin Mahmud, K., Mahayani, N.P.D., Mansor,
956 A., Marshall, A.R., Martin, E.H., Matos, D.C.L., Meave, J.A., Melo, F.P.L., Mendoza,
957 Z.H.A., Metali, F., Medjibe, V.P., Metzger, J.P., Metzker, T., Mohandass, D., Munguía-
958 Rosas, M.A., Muñoz, R., Nurtjahy, E., De Oliveira, E.L., Onrizal, Parolin, P., Parren, M.,
959 Parthasarathy, N., Paudel, E., Perez, R., Pérez-García, E.A., Pommer, U., Poorter, L.,
960 Qi, L., Piedade, M.T.F., Pinto, J.R.R., Poulsen, A.D., Poulsen, J.R., Powers, J.S.,
961 Prasad, R.C., Puyravaud, J.-P., Rangel, O., Reitsma, J., Rocha, D.S.B., Rolim, S.,
962 Rovero, F., Rozak, A., Ruokolainen, K., Rutishauser, E., Rutten, G., Mohd Said, M.N.,
963 Saiter, F.Z., Saner, P., Santos, B., Dos Santos, J.R., Sarker, S.K., Schmitt, C.B.,
964 Schoengart, J., Schulze, M., Sheil, D., Sist, P., Souza, A.F., Spironello, W.R., Sposito,
965 T., Steinmetz, R., Stevart, T., Suganuma, M.S., Sukri, R., Sultana, A., Sukumar, R.,
966 Sunderland, T., Supriyadi, Suresh, H.S., Suzuki, E., Tabarelli, M., Tang, J., Tanner,
967 E.V.J., Targhetta, N., Theilade, I., Thomas, D., Timberlake, J., De Morisson Valeriano,
968 M., Van Valkenburg, J., Van Do, T., Van Sam, H., Vandermeer, J.H., Verbeeck, H.,
969 Vetaas, O.R., Adekunle, V., Vieira, S.A., Webb, C.O., Webb, E.L., Whitfeld, T., Wich, S.,
970 Williams, J., Wiser, S., Wittmann, F., Yang, X., Yao, C.Y.A., Yap, S.L., Zahawi, R.A.,
971 Zakaria, R. & Zang, R. (2018) Phylogenetic classification of the world's tropical forests.
972 *Proceedings of the National Academy of Sciences of the United States of America*, **115**.
973 Slik, J.W.F., Paoli, G., McGuire, K., Amaral, I., Barroso, J., Bastian, M., Blanc, L., Bongers,
974 F., Boundja, P., Clark, C., Collins, M., Dauby, G., Ding, Y., Doucet, J.-L., Eler, E.,
975 Ferreira, L., Forshed, O., Fredriksson, G., Gillet, J.-F., Harris, D., Leal, M., Laumonier,
976 Y., Malhi, Y., Mansor, A., Martin, E., Miyamoto, K., Araujo-Murakami, A., Nagamasu, H.,
977 Nilus, R., Nurtjahya, E., Oliveira, Á., Onrizal, O., Parada-Gutierrez, A., Permana, A.,
978 Poorter, L., Poulsen, J., Ramirez-Angulo, H., Reitsma, J., Rovero, F., Rozak, A., Sheil,
979 D., Silva-Espejo, J., Silveira, M., Spironelo, W., ter Steege, H., Stevart, T., Navarro-
980 Aguilar, G.E., Sunderland, T., Suzuki, E., Tang, J., Theilade, I., van der Heijden, G., van
981 Valkenburg, J., Van Do, T., Vilanova, E., Vos, V., Wich, S., Wöll, H., Yoneda, T., Zang,
982 R., Zhang, M.-G. & Zweifel, N. (2013) Large trees drive forest aboveground biomass

variation in moist lowland forests across the tropics. *Global Ecology and Biogeography*, **22**, 1261–1271.

Stark, S.C., Enquist, B.J., Saleska, S.R., Leitold, V., Schietti, J., Longo, M., Alves, L.F., Camargo, P.B. & Oliveira, R.C. (2015) Linking canopy leaf area and light environments with tree size distributions to explain Amazon forest demography. *Ecology Letters*, **18**, 636–645.

Stark, S.C., Leitold, V., Wu, J.L., Hunter, M.O., de Castilho, C. V., Costa, F.R.C., Mcmahon, S.M., Parker, G.G., Shimabukuro, M.T., Lefsky, M.A., Keller, M., Alves, L.F., Schietti, J., Shimabukuro, Y.E., Brand??o, D.O., Woodcock, T.K., Higuchi, N., de Camargo, P.B., de Oliveira, R.C. & Saleska, S.R. (2012) Amazon forest carbon dynamics predicted by profiles of canopy leaf area and light environment. *Ecology Letters*, **15**, 1406–1414.

Stegen, J.C., Swenson, N.G., Enquist, B.J., White, E.P., Phillips, O.L., Jørgensen, P.M., Weiser, M.D., Monteagudo Mendoza, A. & Núñez Vargas, P. (2011) Variation in above-ground forest biomass across broad climatic gradients. *Global Ecology and Biogeography*, **20**, 744–754.

Sullivan, M.J.P., Talbot, J., Lewis, S.L., Phillips, O.L., Qie, L., Begne, S.K., Chave, J., Cuni-Sanchez, A., Hubau, W., Lopez-Gonzalez, G., Miles, L., Monteagudo-Mendoza, A., Sonké, B., Sunderland, T., Ter Steege, H., White, L.J.T., Affum-Baffoe, K., Aiba, S.-I., De Almeida, E.C., De Oliveira, E.A., Alvarez-Loayza, P., Dávila, E.Á., Andrade, A., Aragão, L.E.O.C., Ashton, P., Aymard, G.A., Baker, T.R., Balinga, M., Banin, L.F., Baraloto, C., Bastin, J.-F., Berry, N., Bogaert, J., Bonal, D., Bongers, F., Brienen, R., Camargo, J.L.C., Cerón, C., Moscoso, V.C., Chezeaux, E., Clark, C.J., Pacheco, Á.C., Comiskey, J.A., Valverde, F.C., Coronado, E.N.H., Dargie, G., Davies, S.J., De Canniere, C., Djuikouo, M.N., Doucet, J.-L., Erwin, T.L., Espejo, J.S., Ewango, C.E.N., Fauset, S., Feldpausch, T.R., Herrera, R., Gilpin, M., Gloor, E., Hall, J.S., Harris, D.J., Hart, T.B., Kartawinata, K., Kho, L.K., Kitayama, K., Laurance, S.G.W., Laurance, W.F., Leal, M.E., Lovejoy, T., Lovett, J.C., Lukasu, F.M., Makana, J.-R., Malhi, Y., Maracahipes, L., Marimon, B.S., Junior, B.H.M., Marshall, A.R., Morandi, P.S., Mukendi,

J.T., Mukinzi, J., Nilus, R., Vargas, P.N., Camacho, N.C.P., Pardo, G., Peña-Claros, M., Pétronelli, P., Pickavance, G.C., Poulsen, A.D., Poulsen, J.R., Primack, R.B., Priyadi, H., Quesada, C.A., Reitsma, J., Réjou-Méchain, M., Restrepo, Z., Rutishauser, E., Salim, K.A., Salomão, R.P., Samsoedin, I., Sheil, D., Sierra, R., Silveira, M., Slik, J.W.F., Steel, L., Taedoumg, H., Tan, S., Terborgh, J.W., Thomas, S.C., Toledo, M., Umunay, P.M., Gamarra, L.V., Vieira, I.C.G., Vos, V.A., Wang, O., Willcock, S. & Zemagho, L. (2017) Diversity and carbon storage across the tropical forest biome. *Scientific Reports*, **7**.

Tang, H. & Dubayah, R. (2017) Light-driven growth in Amazon evergreen forests explained by seasonal variations of vertical canopy structure. *Proceedings of the National Academy of Sciences of the United States of America*, **114**, 2640–2644.

Thomas, R.Q., Kellner, J.R., Clark, D.B. & Peart, D.R. (2013) Low mortality in tall tropical trees. *Ecology*, **94**, 920–929.

West, G.B., Enquist, B.J., Brown, J.H., West, G.B., Brown, J.H., Enquist, B.J. & Brown, J.H. (2009) Extensions and evaluations of a general quantitative theory of forest structure and dynamics. *Proceedings of the National Academy of Sciences of the United States of America*, **106**, 7040–7045.

Zanne, A.E., Lopez-Gonzalez, G., Coomes, D.A., Ilic, J., Jansen, S., Lewis, S.L., Miller, R.B., Swenson, N.G., Wiemann, M.C. & Chave, J. (2009) Global wood density database. *Dryad*, **235**, 33.

Supplementary information.

Supplementary table 1. Plot, Site and PIs

Supplementary table 2. Coefficients of plot level structure prediction from the *ith* largest trees.

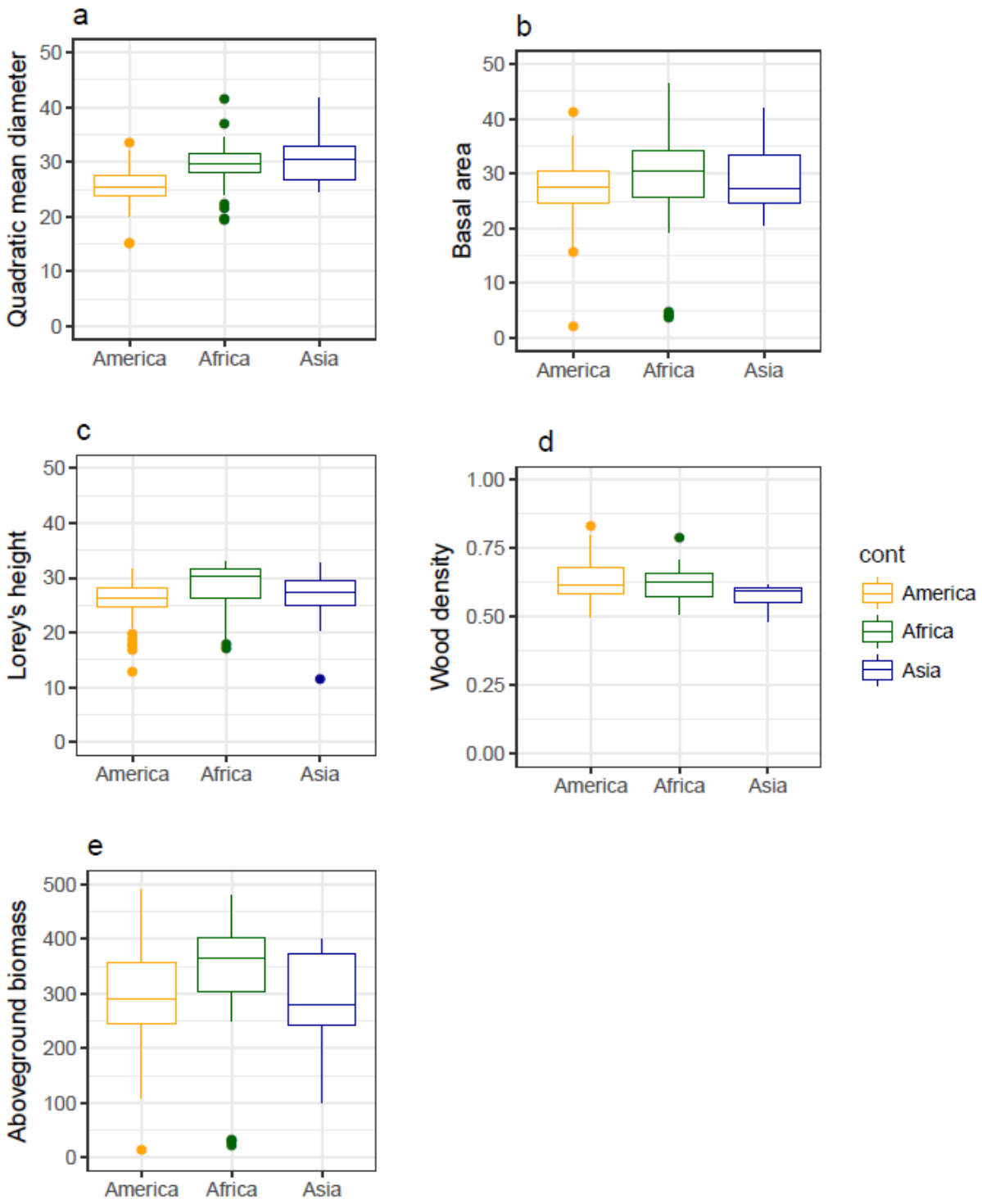

Supplementary figure 1. Cross-continent comparison of plot-metrics distribution averaged at the site level. Figures illustrates respectively the distribution of the values for the quadratic mean diameter (a), basal area (b), Lorey's height (c), wood density (d) and aboveground biomass (e).

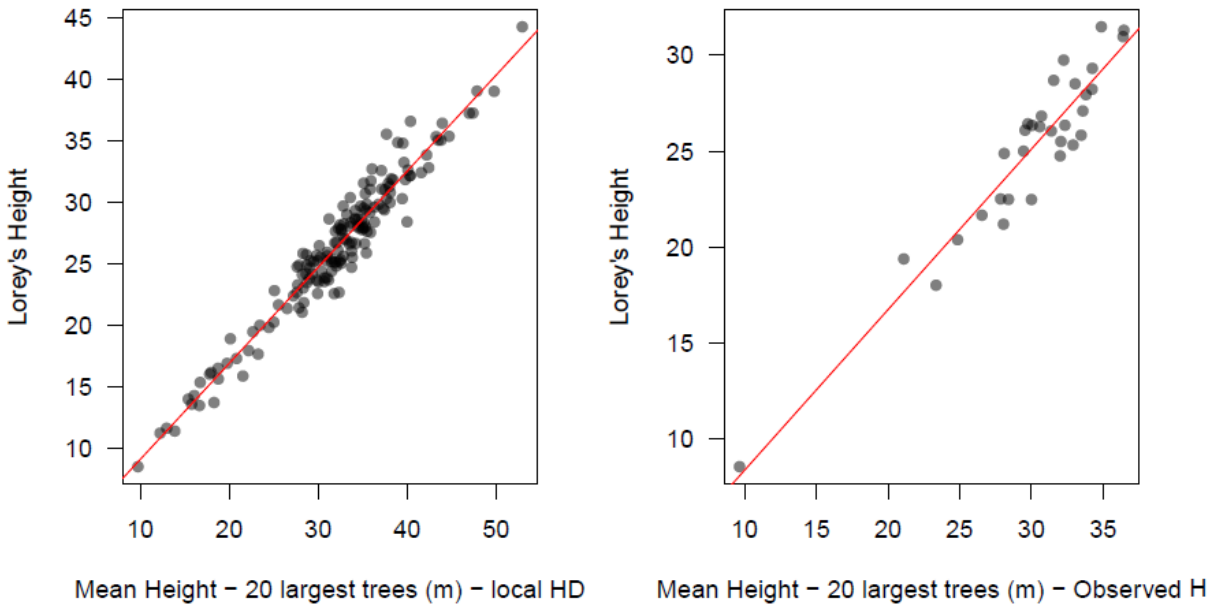

Supplementary figure 2. Lorey's Height prediction from the 20 largest trees. Figures show the results using (i) local D-H allometries for 20 sites (left subfigure) and (ii) using plots where height is measured on all trees in Malebo site in the Democratic Republic of the Congo (right subfigure).

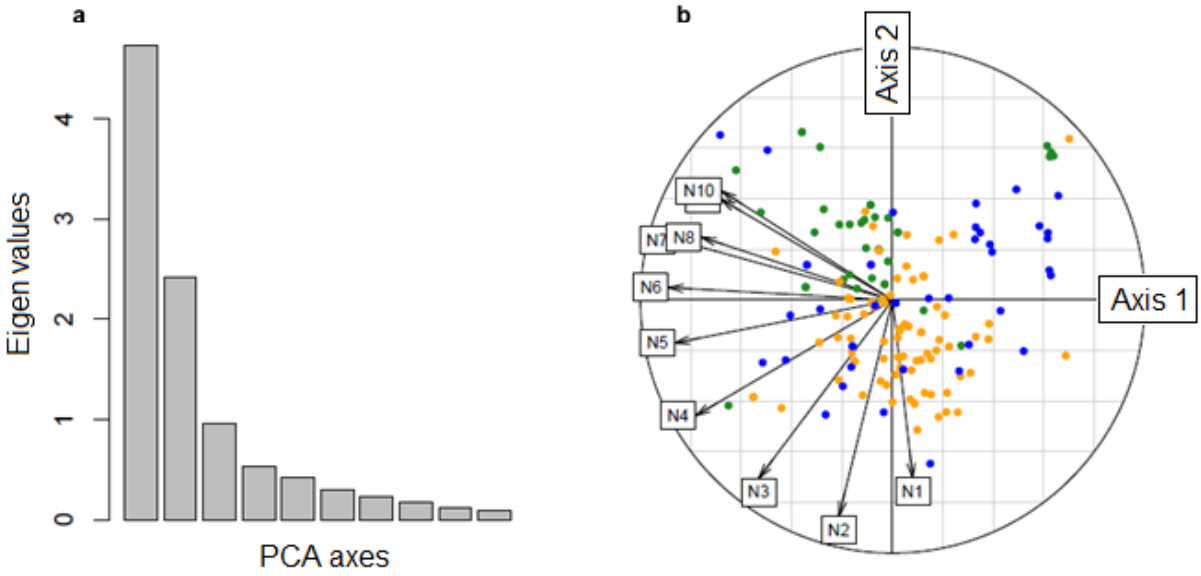

Supplementary figure 3. PCA on the diameter structure and corresponding mean distribution for high contributions of axis 1 and axis 2. (A) Illustration of top and low percentile observed for each axis, with diameter distributions represented as the relative difference with the average observed distribution.(B) Biplot with contribution to the PCA of all the diameter classes, with the respective position of each site in the space defined by axis1 and 2. Axis 1 is driven by differences in global abundance of trees and axis 2 is driven by a difference of balance between abundance of small vs. large trees. Colors represent continent, with Africa, America and Asia respectively in green, orange and blue.

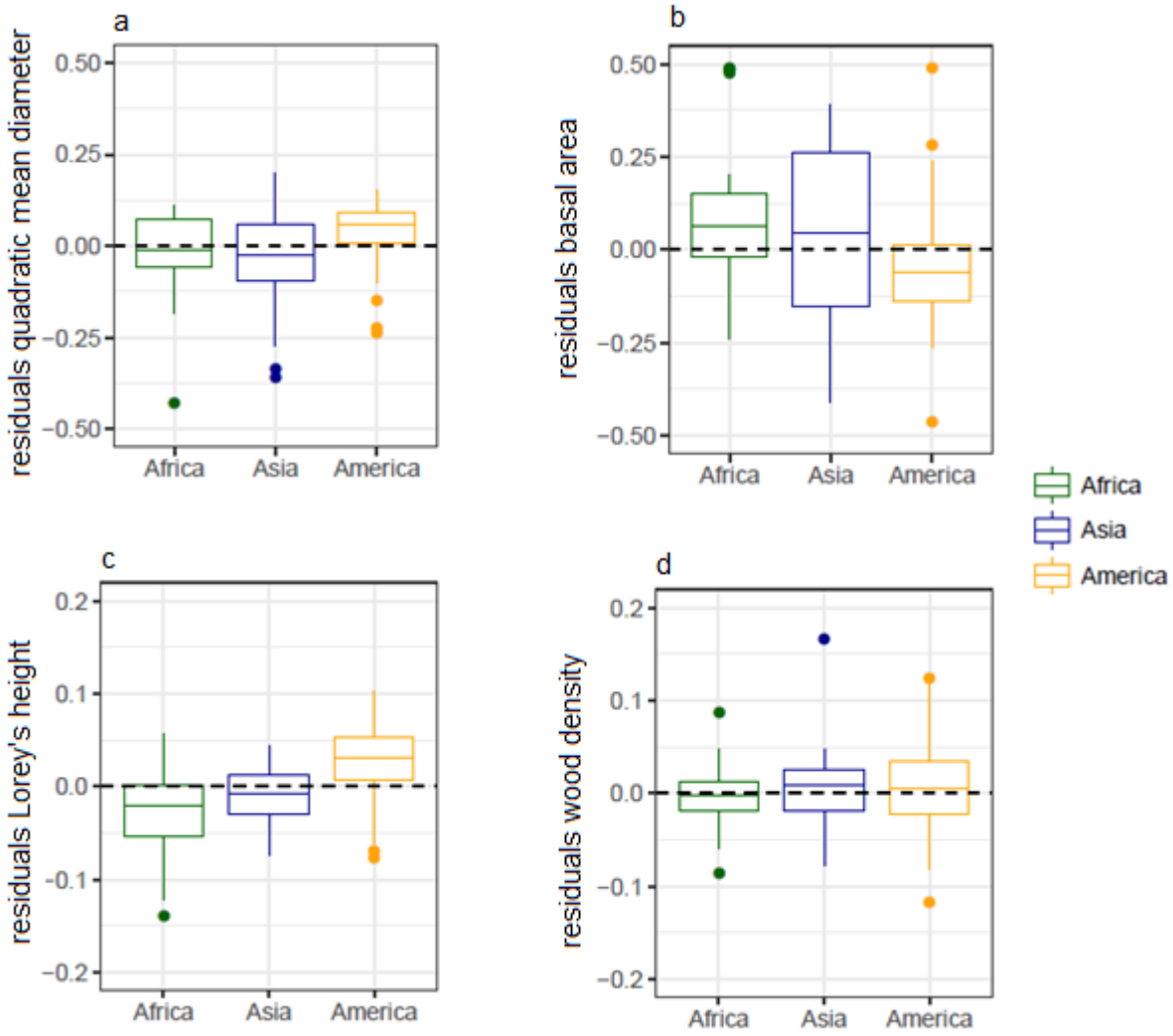

Supplementary figure 4. Cross-continent comparison of the relative residuals from the prediction of plot-metrics from the 20 largest trees. The relative residuals are generally low (<10%). Systematic small differences can however be found in America, where the quadratic mean diameter and Lorey's height tend to be slightly overestimated and the basal area slightly underestimated.